KIT Meeting on Composition
21 – 23 September 2015

Benefits and prospects of using data from historic projects

Alan Watson
University of Leeds
a.a.watson@leeds.ac.uk

The text for today's sermon

"Theories crumble but good observations never fade"

Harlow Shapley (Mount Wilson and Harvard Observatory astronomer)

Clearly, if there are good data from historic projects, it is common sense to try to exploit them – economics, timescale…….

Guidance from Andreas:

"One goal of the workshop is to discuss if the limitations in understanding the composition and origin of cosmic rays is mainly coming from the measurements, the astrophysical models, or from the hadronic interaction models.

Therefore, concentrate on the systematics of your results."

I'm sure this applies to modellers and experimentalists

In my view, systematic uncertainties in hadronic models are fundamentally unknowable - in the absence of machine results – so they will often dominate. Thus test models against as wide a range of data as possible.

Successes:

1. Use of Haverah Park data to set upper limits on photon fluxes above 10^{19} eV

Work, jointly with the Santiago de Compostela group, began as an effort to understand the backgrounds against which we had to search for neutrino signals

Led to development of methods to analyse very inclined events now used at Auger and to important photon limits

VOLUME 85, NUMBER 11 PHYSICAL REVIEW LETTERS 11 SEPTEMBER 2000

New Constraints from Haverah Park Data on the Photon and Iron Fluxes of Ultrahigh-Energy Cosmic Rays

M. Ave,[1] J. A. Hinton,[2] R. A. Vázquez,[1] A. A. Watson,[2] and E. Zas[1]
[1]*Departamento de Física de Partículas, Universidad de Santiago, 15706 Santiago de Compostela, Spain*
[2]*Department of Physics and Astronomy, University of Leeds, Leeds LS2 9JT, United Kingdom*
(Received 16 March 2000; revised manuscript received 8 August 2000)

Using data from inclined events ($60° < \theta < 80°$) recorded by the Haverah Park shower detector, we show that above 10^{19} eV less than 41% (54%) of the primary cosmic rays can be photons (iron nuclei) at the 95% confidence level. Above 4×10^{19} eV less than 65% of the cosmic rays can be photonic at the same confidence level. These limits place important constraints on some models of the origin of ultrahigh-energy cosmic rays. Details of two new events above 10^{20} eV are reported.

60 EeV, 74°

Archiving of data crucial

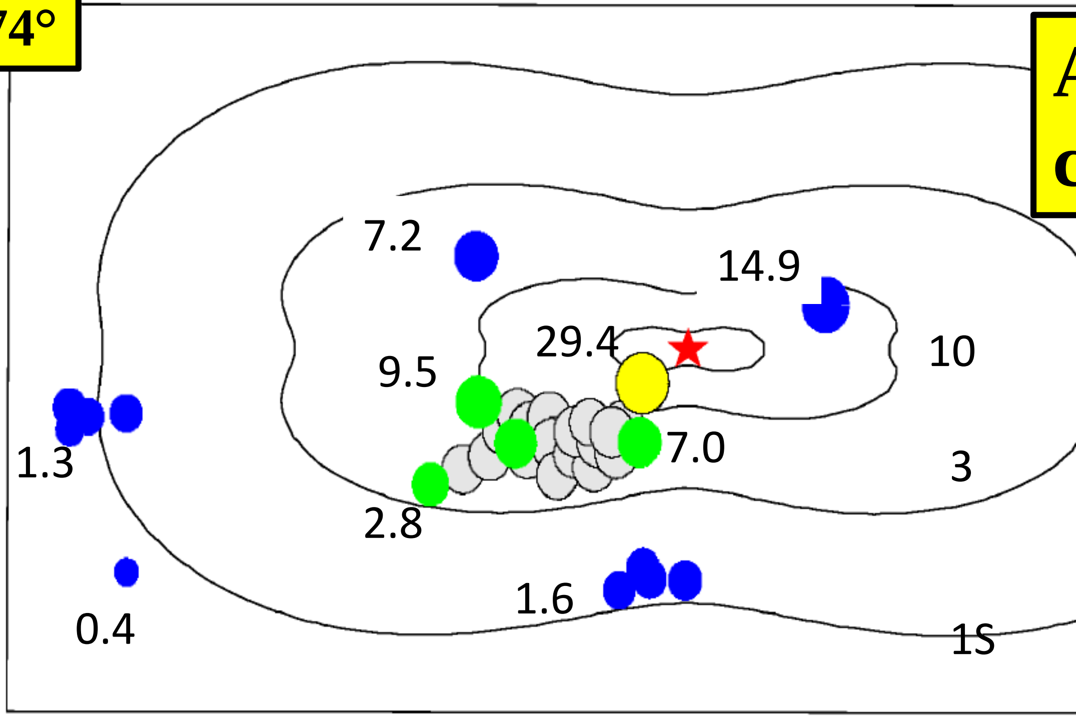

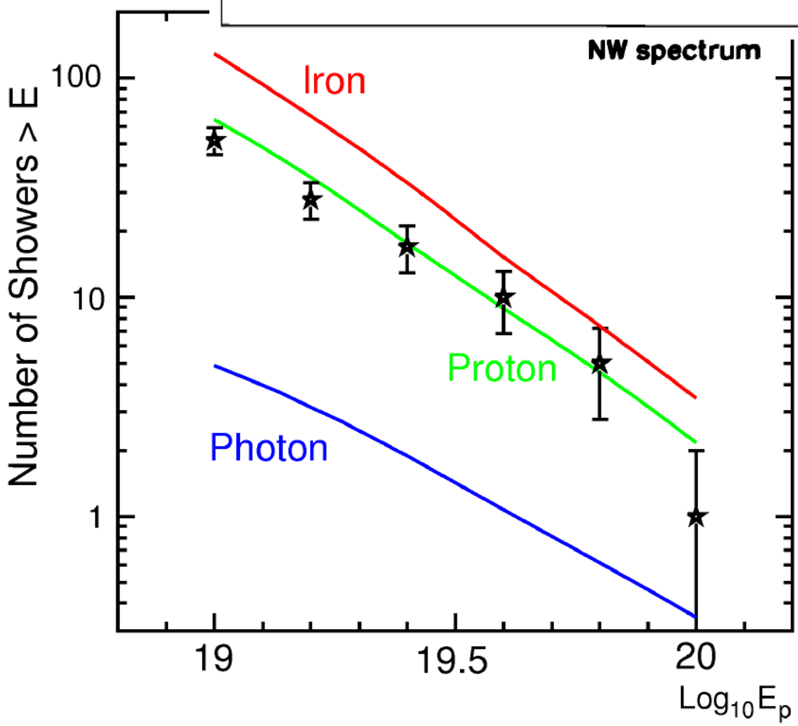

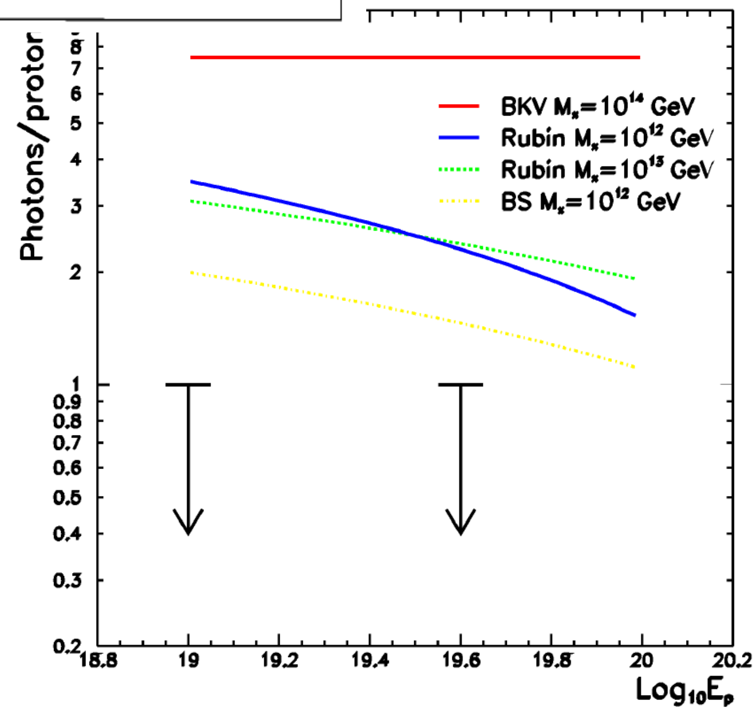

Successes:

2. Use of Haverah Park measurement on lateral distribution to make mass estimates from 2 x 10^{17} to 3 x 10^{18} eV

ELSEVIER

Astroparticle Physics 19 (2003) 61–75

www.elsevier.com/locate/a:

Mass composition of cosmic rays in the range 2×10^{17}–3×10^{18} eV measured with the Haverah Park array

M. Ave [a,*], L. Cazón [b], J.A. Hinton [a,1], J. Knapp [a], J. Lloyd-Evans [a], A.A. Watson [a]

[a] *Department of Physics and Astronomy, University of Leeds, Leeds LS2 9JT, UK*
[b] *Dept. de Física de Partículas, Universidad de Santiago, 15706 Santiago de Compostela, Spain*

Received 18 December 2001; accepted 11 March 2002

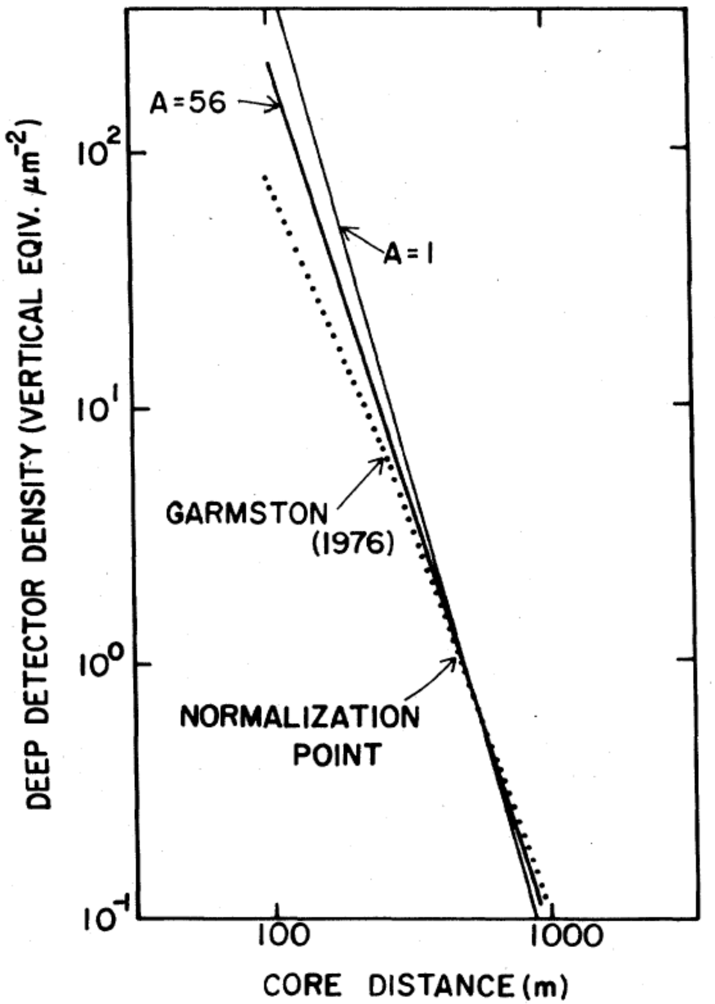

FIG. 14. The average lateral distribution for the respon[se of] the Haverah Park deep-water detectors. The solid lines [are] calculations, the dotted line data.

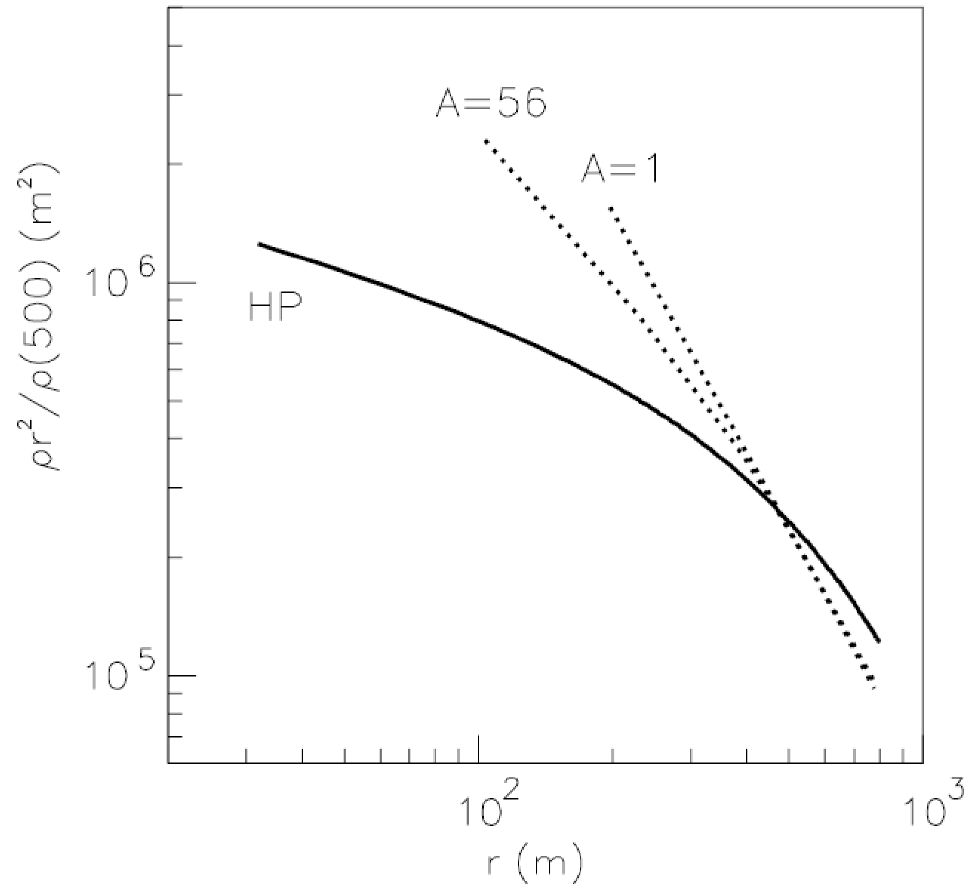

Fig. 2. A comparison of Haverah Park data and the calculations for p and Fe induced showers from [5]. ρ is the water-Cherenkov signal.

[5] **Gaisser et al Rev Mod Phys 1978**

- the days of Feynman scaling!

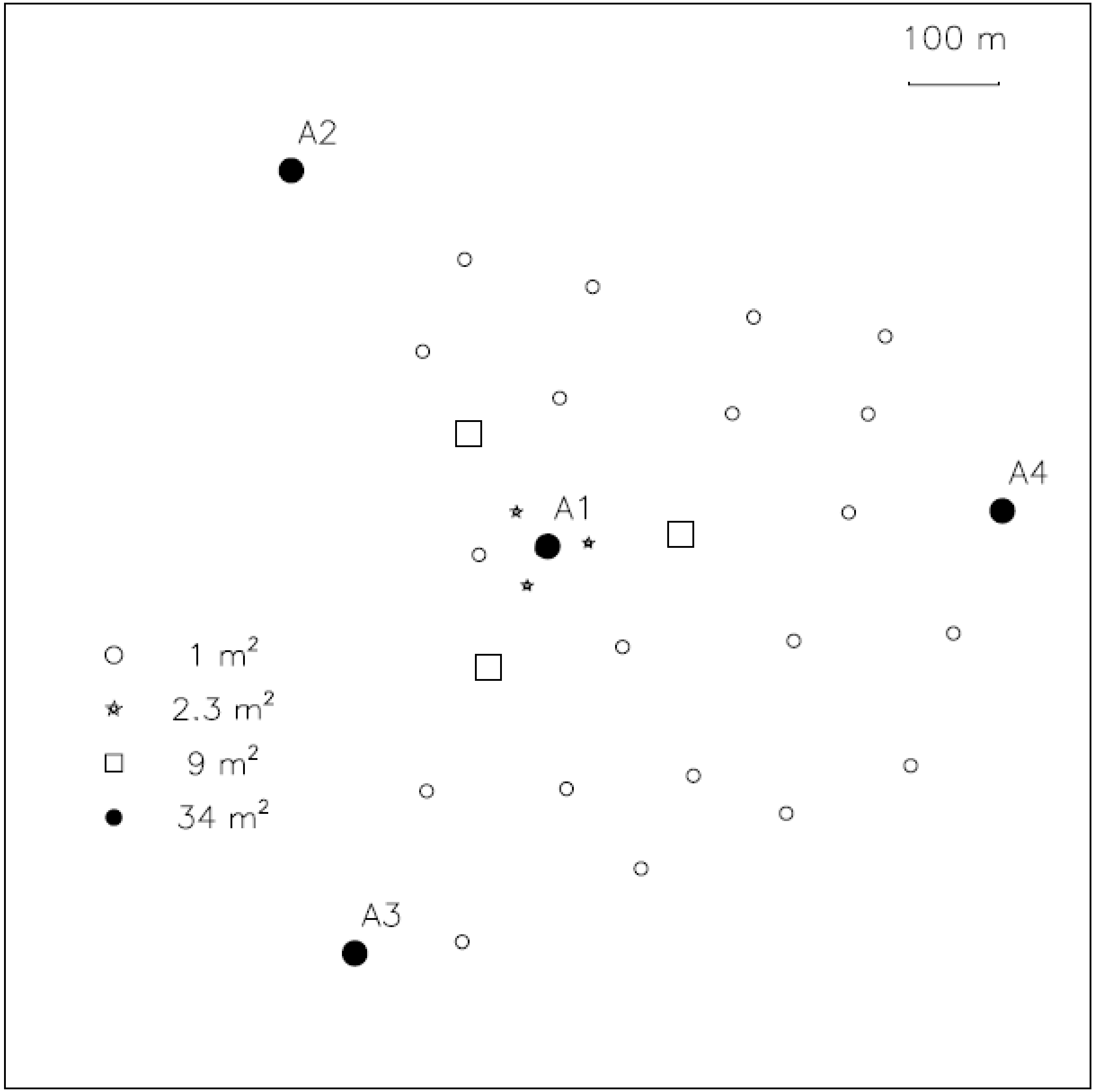

Fig. 1. The inner part of the Haverah Park array, the so called infill array.

Slope parameter defined by $\rho(r) = kr^{(\eta + r/4000)}$

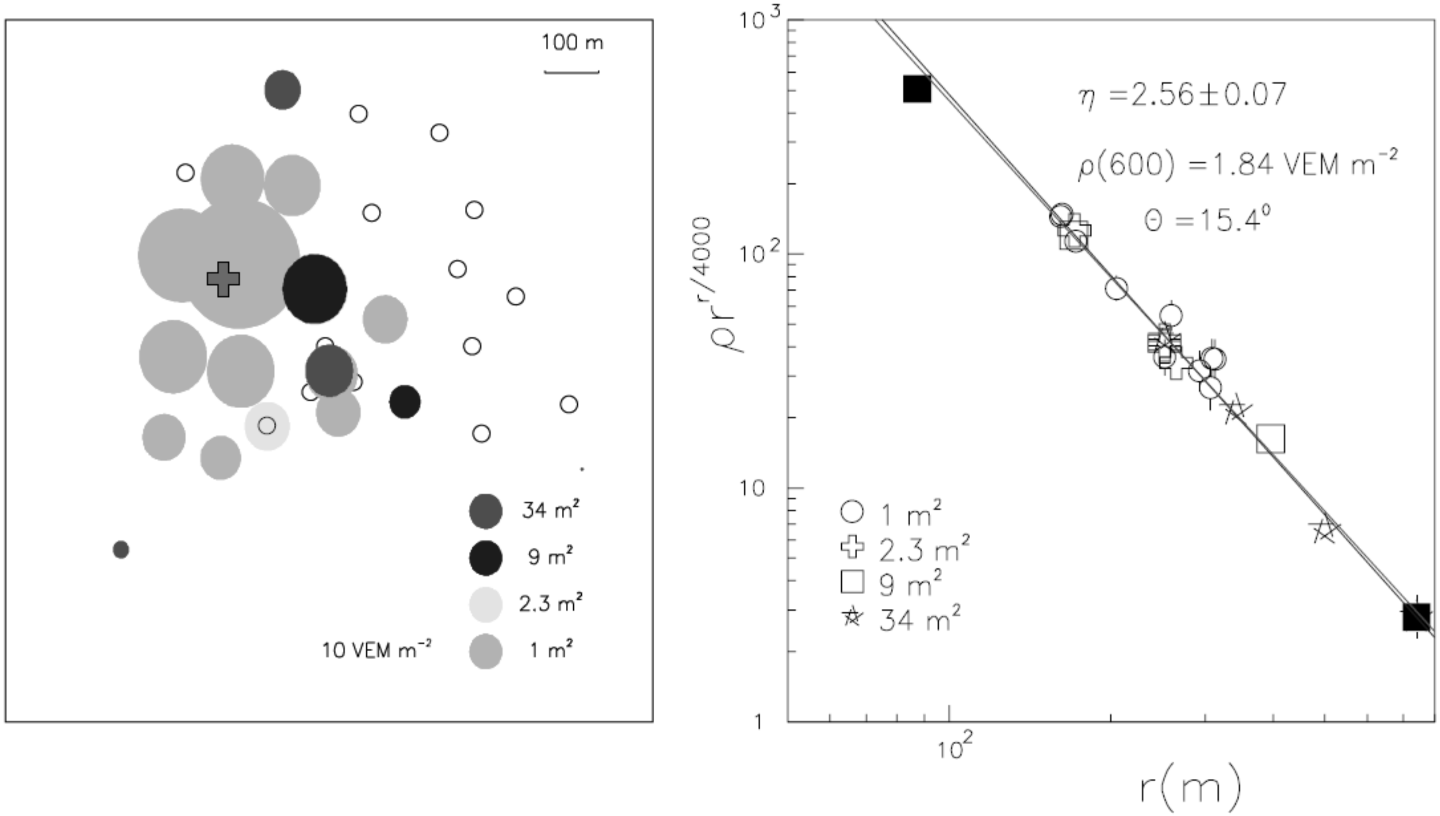

Fig. 4. Example of the reconstruction of an infill event. Left panel: projection of the array into the shower plane with recorded densities shown as circles with radius proportional to the logarithm of the density. The detector areas are indicated by grey scales. The detectors are displayed in the plane perpendicular to the shower axis. Right panel: fitted lateral distribution function. The two lines correspond to the lateral distribution function as obtained with ringing analysis and with the method described in the text. The difference in the value of η for this particular event is 0.04. The abscissa shows a quantity that linearises the lateral distribution function given in Eq. (1). Filled symbols indicate detectors with signals above saturation or below threshold.

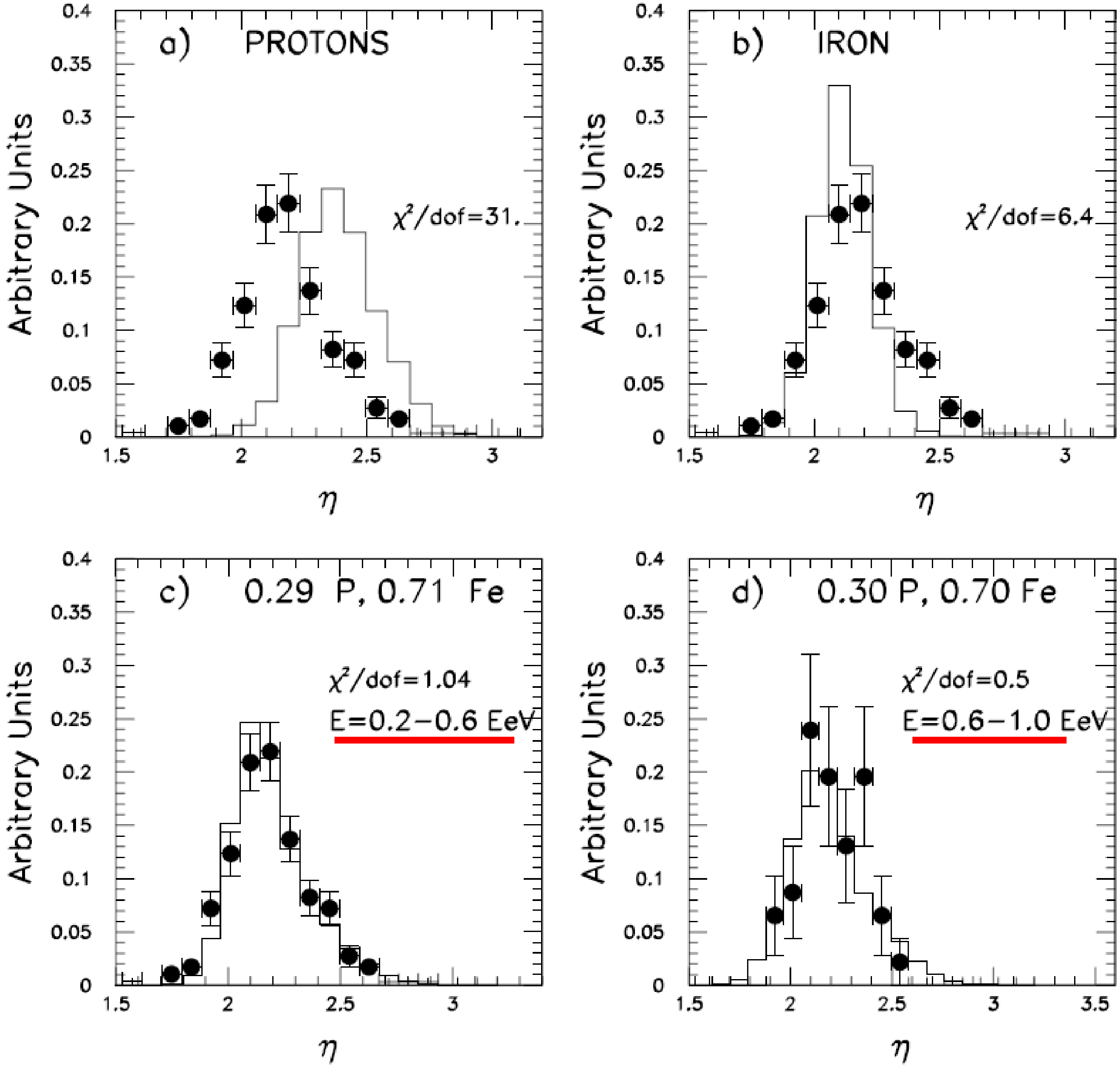

Fig. 7. Distributions of η for experimental data, and model predictions with different primary masses.

QGSJET98

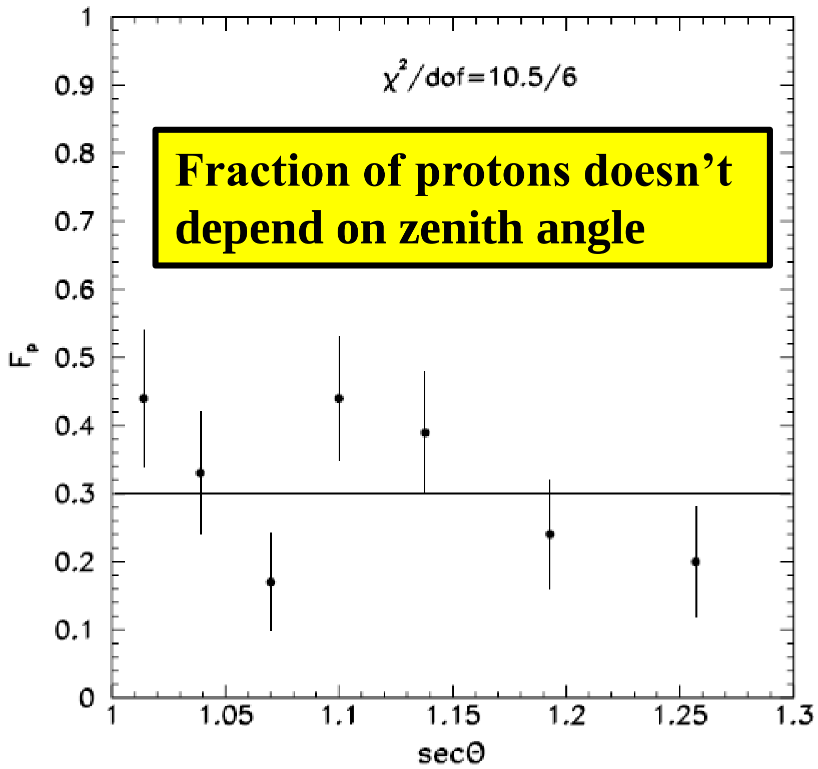

Fig. 10. Predicted value of F_p in the energy range 0.3–0.5 EeV for different zenith angle bins. The predicted value of F_p does not depend on zenith angle.

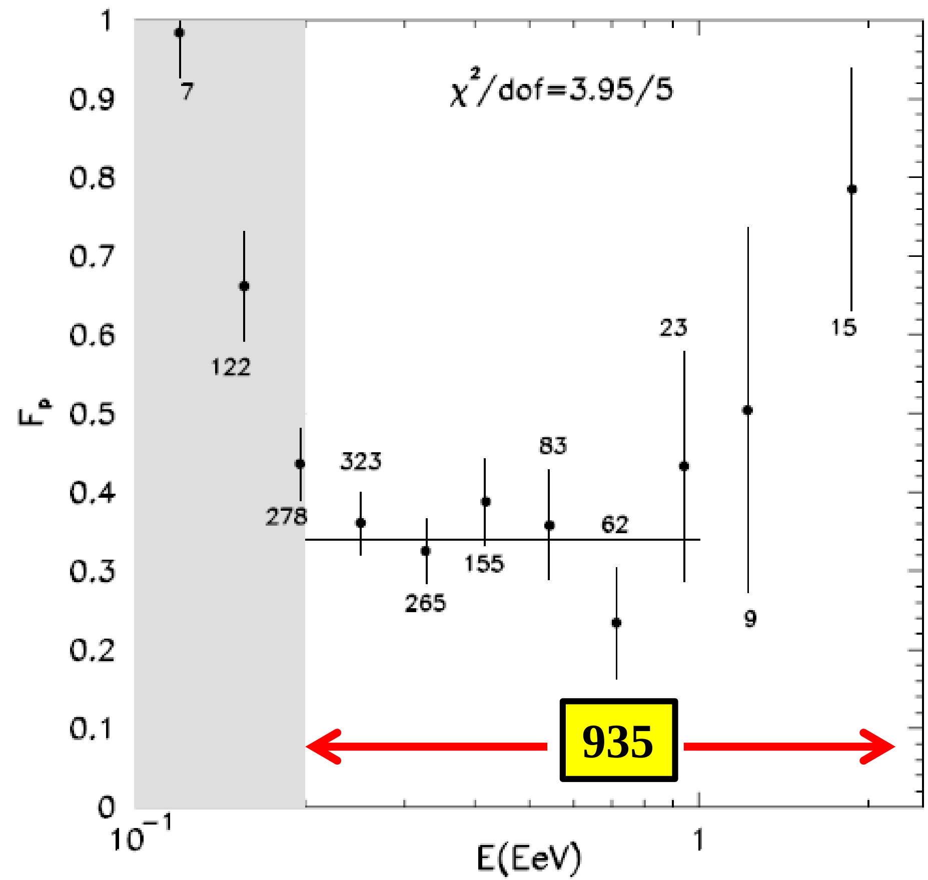

Fig. 11. Predicted value of F_p as a function of the energy. A fit to a constant composition in the energy range 0.2–1.0 EeV is also shown with its corresponding χ^2. The number of events in each energy bin is shown. The shadow region corresponds to the energy range in which the analysis is affected by trigger biases (see text).

Analysis made using QGSJET98

Not so successful – data not archived

ELSEVIER

Astroparticle Physics 21 (2004) 597–607

www.elsevier.com/locate/astropart

The mass composition of cosmic rays near 10^{18} eV as deduced from measurements made at Volcano Ranch

M.T. Dova [a], M.E. Manceñido [a], A.G. Mariazzi [a], T.P. McCauley [b], A.A. Watson [c,*]

[a] Instituto de Fisica, CONICET, Dto. de Fisica, Universidad Nacional de La Plata, C.C.67, 1900 La Plata, Argentina

[b] Department of Physics, Northeastern University, Boston, MA 02115, USA

[c] School of Physics and Astronomy, University of Leeds, Leeds LS2 9JT, UK

Received 4 September 2003; received in revised form 7 April 2004; accepted 16 April 2004

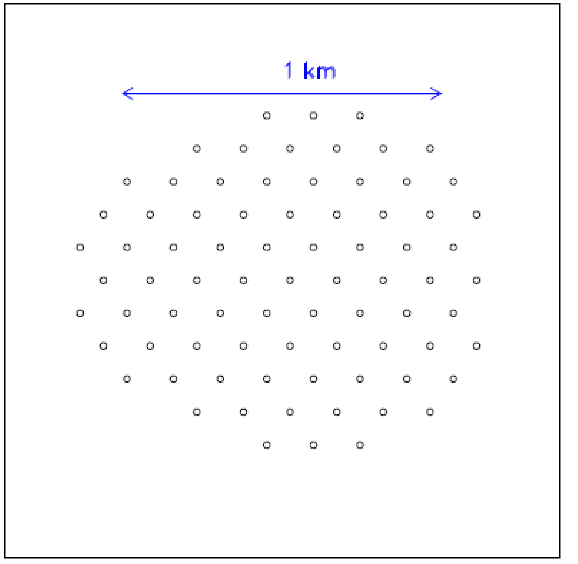

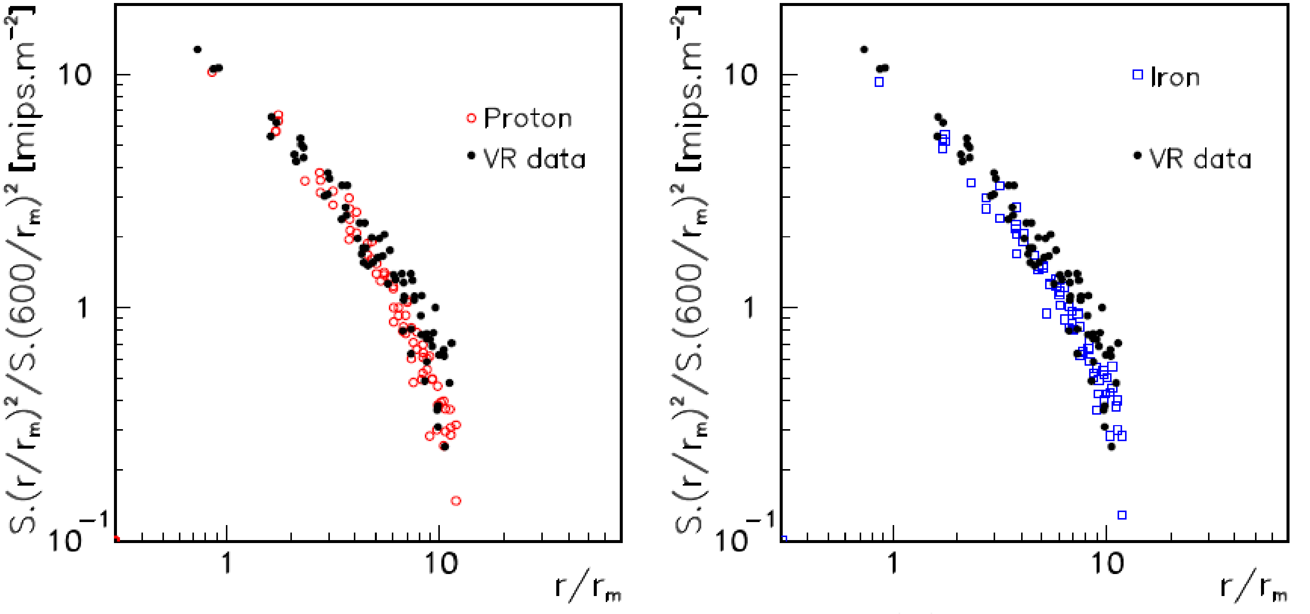

FIG. 3. Comparison between lateral distribution measurements in a single event [24] and the simulated scintillator response

ι the configuration of VR array for $10^{19.1}$ eV proton and iron showers.

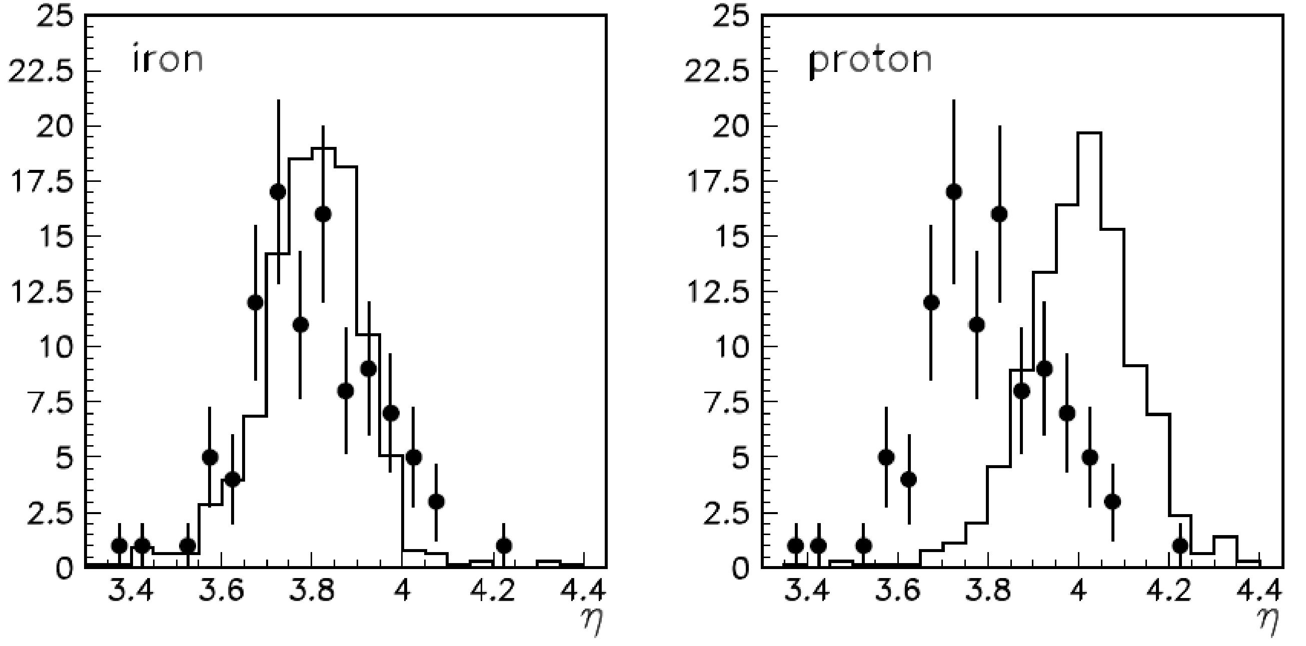

FIG. 6. The measured distributions of η (data points) with histograms from Monte Carlo calculations of pure iron (left) and pure proton (right) with $1.0 < \sec\theta < 1.1$, using QGSJET98.

366 events for which LDF had been found with high precision - but energies not known for each event

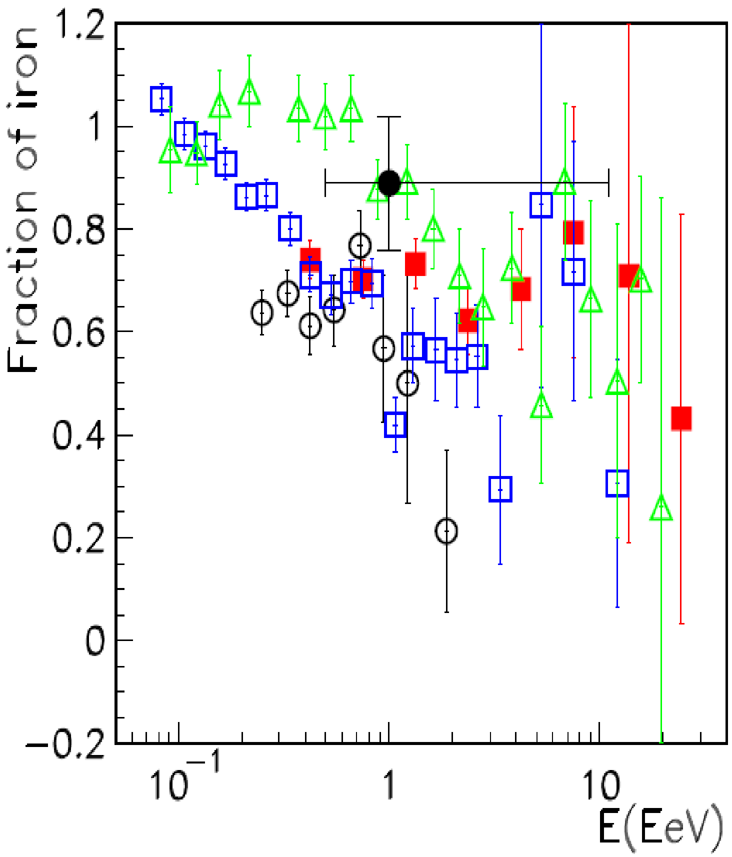

188 FIG. 8. Fe fraction from various experiments: Fly's Eye (△), Agasa A100 (■), Agasa A1 (□) using SIBYLL 1.5 ([6] and references therein) and Haverah Park [1], using QGSJET98 (○)). Mean composition determined in this paper with the corresponding error for the Volcano Ranch energy range using QGSJET98 (●) is shown.

The Muon Problem

Predictions from models, with p – Fe composition, are unable to match observed density of muons in Auger studies – though the introduction of the ρ does seem to help

Too few muons are/were predicted: e.g. in very inclined showers

Worth testing these using other data:

- **Different methods of measurement**
- **Different energies of primaries**
- **Different altitudes**

Data from Akeno/AGASA and Haverah Park may be useful here

Hayashida et al. J Phys G 21 1101- 1119 1995: a very detailed paper

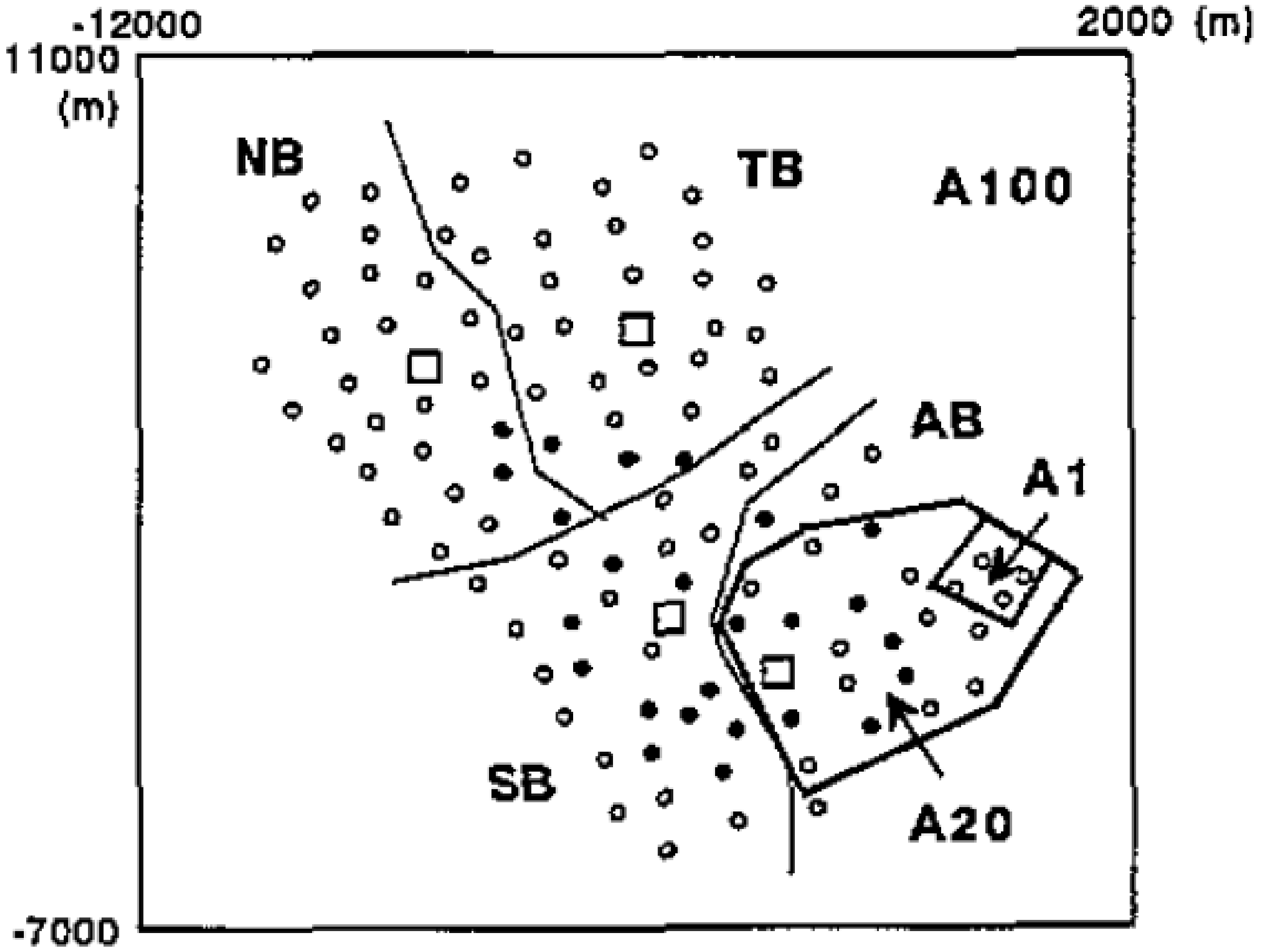

Depth = 920 g cm^{-2} : Cannot, of course, use Auger simulations at 18º

Akeno/AGASA muon data:

Proportional counters under concrete

- (on-off) density from number of counters
- analogue density from calibration with vertical muon (Landau tail, factor of 1.6 beyond 10 m)

Table 1. The durations and numbers of events analysed in each array.

Array	Duration of the experiment	Number of events	Energy range (eV)
A1	October 1981–July 1992	995 457	3×10^{16}–3×10^{18}
A20	December 1984–July 1992	43 482	3×10^{17}–3×10^{19}
A100	June 1991–April 1993	14 735	3×10^{17}–3×10^{19}

Table 2. The numbers and areas of muon detectors used for the present analysis.

Array	Area of one detector (m^2)	Number of detectors	Length of each PC (m)	Number of PC in each detector	Threshold muon energy (GeV)
A1	25.0	8	5.0	50	1.0
A20	25.0	8	5.0	50	1.0
A100	2.8	12	2.0	14	0.5
	10.0	2	5.0	20	0.5

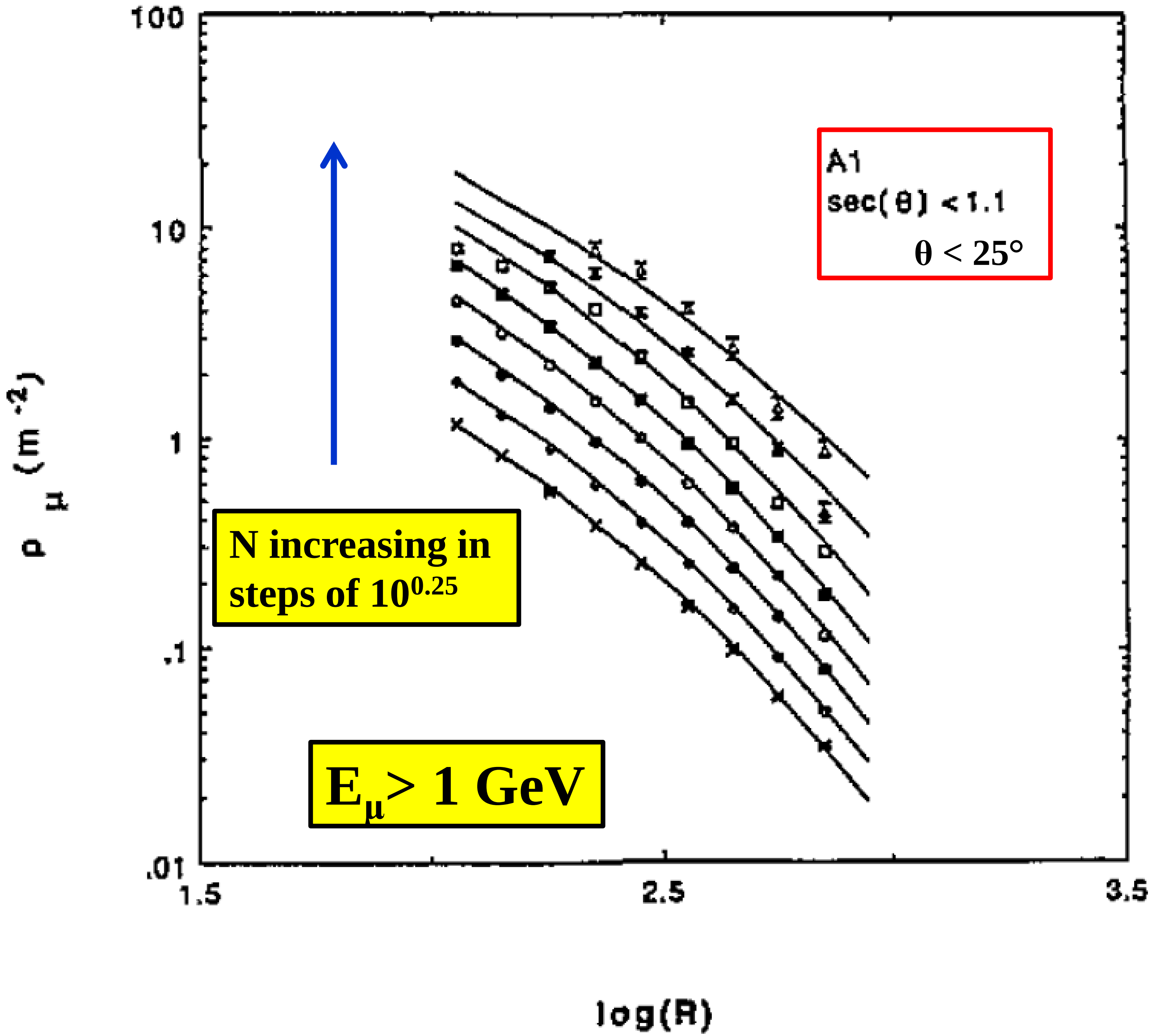

100
10
1
.1
.01
1.5
2.5
3.5
ρ_μ (m^{-2})
log(R)
A1
sec(θ) < 1.1
θ < 25°
N increasing in steps of $10^{0.25}$
E_μ > 1 GeV

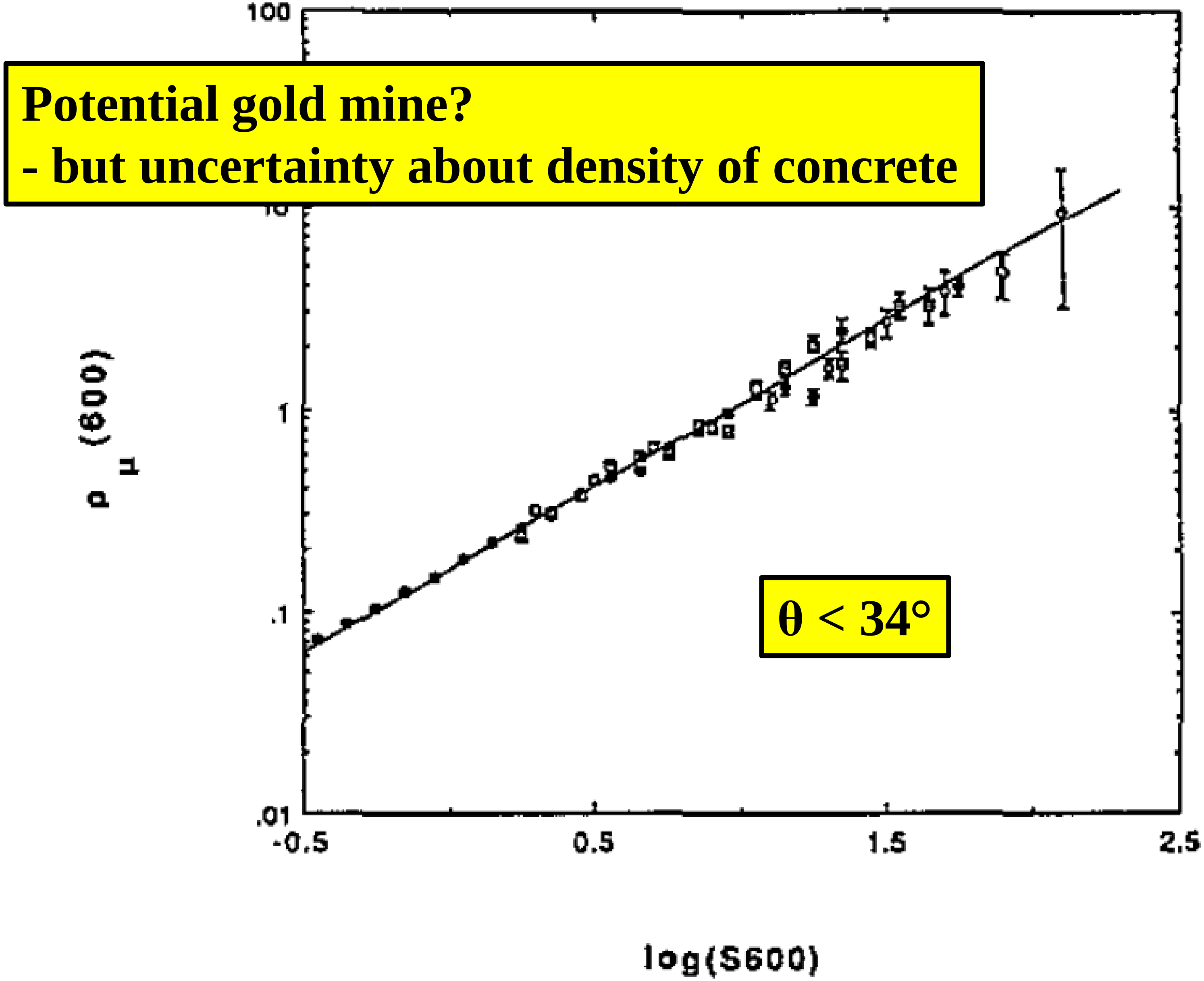

Figure 7. The average $\rho_\mu(600)$ is plotted as a function of $S(600)$ for A1 (closed circle (dotted squares), and A100 (open circles) for vertical showers ($< \sec\theta > = 1.09$). Data A100 are normalized to those from A20. The solid lines represent (8).

Turver et al. (Durham) Muon measurements at Haverah Park

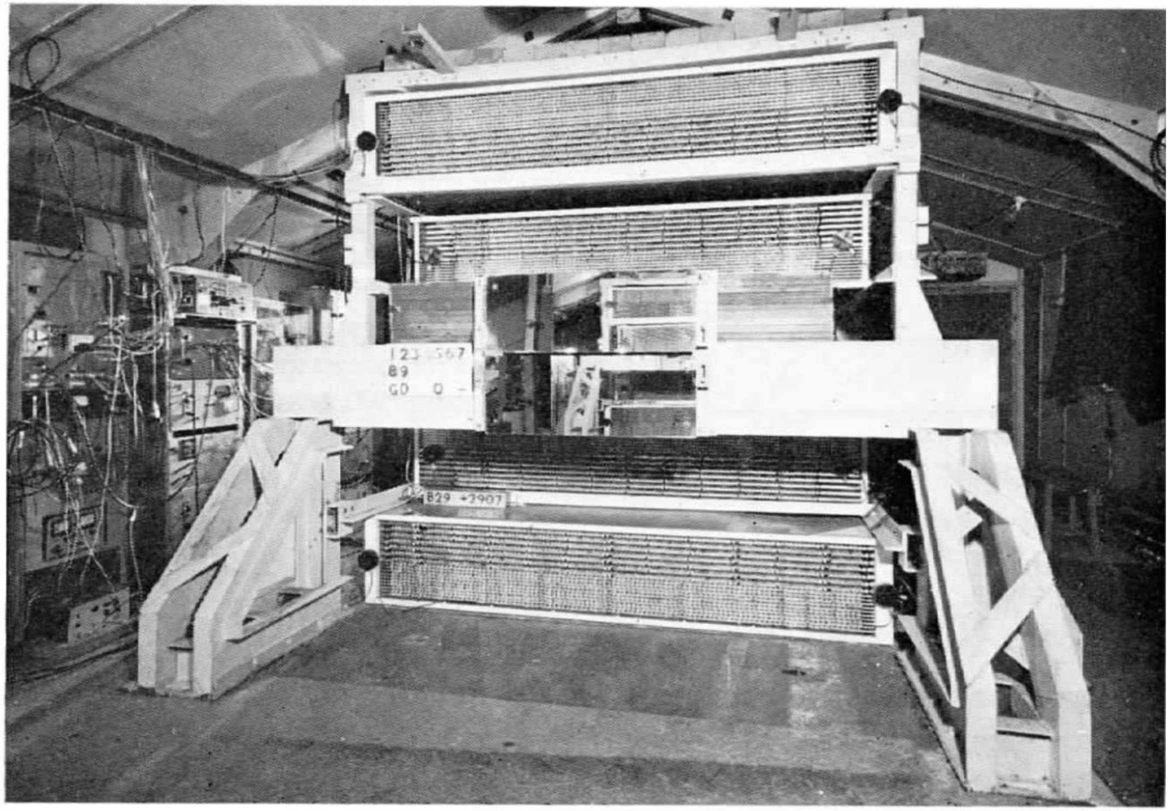

Figure 10. The Haverah Park solid iron magnet spectrograph.

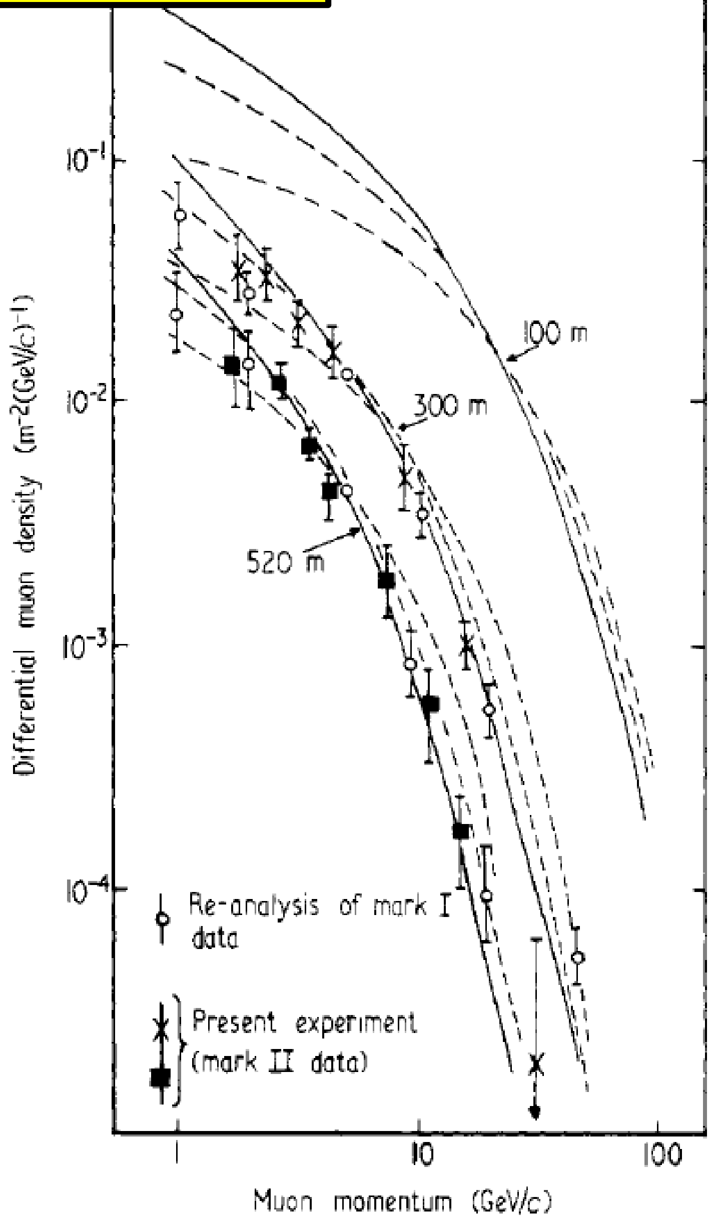

Area = 1.8 m^2 Field = 14.6 kG
Maximum Detectable Momentum = 150 GeV/c
60 cm thickness of Fe from 46 plates

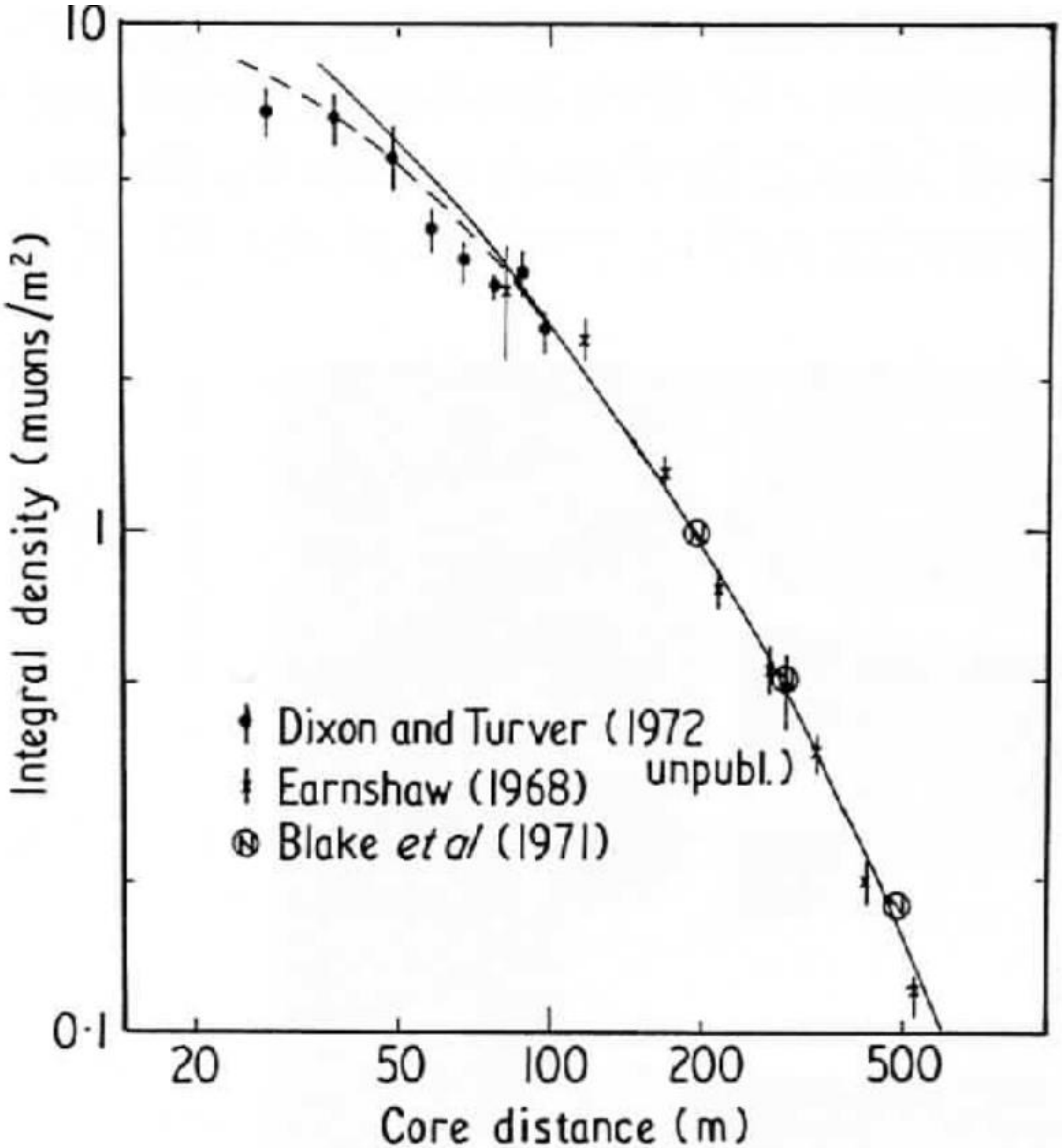

K E Turver: Review article 1970

Muon LDF above 1 GeV

Important data set

Figure 11. The lateral distribution function for muons of energy above 1 GeV in showers of energy $1{\cdot}4 \times 10^{17}$ eV incident at zenith angles less than 40°. The solid line represents the relation given in the text; the broken line shows the expected effect of core location uncertainties of ± 20 m (after A A Watson 1972 private communication).

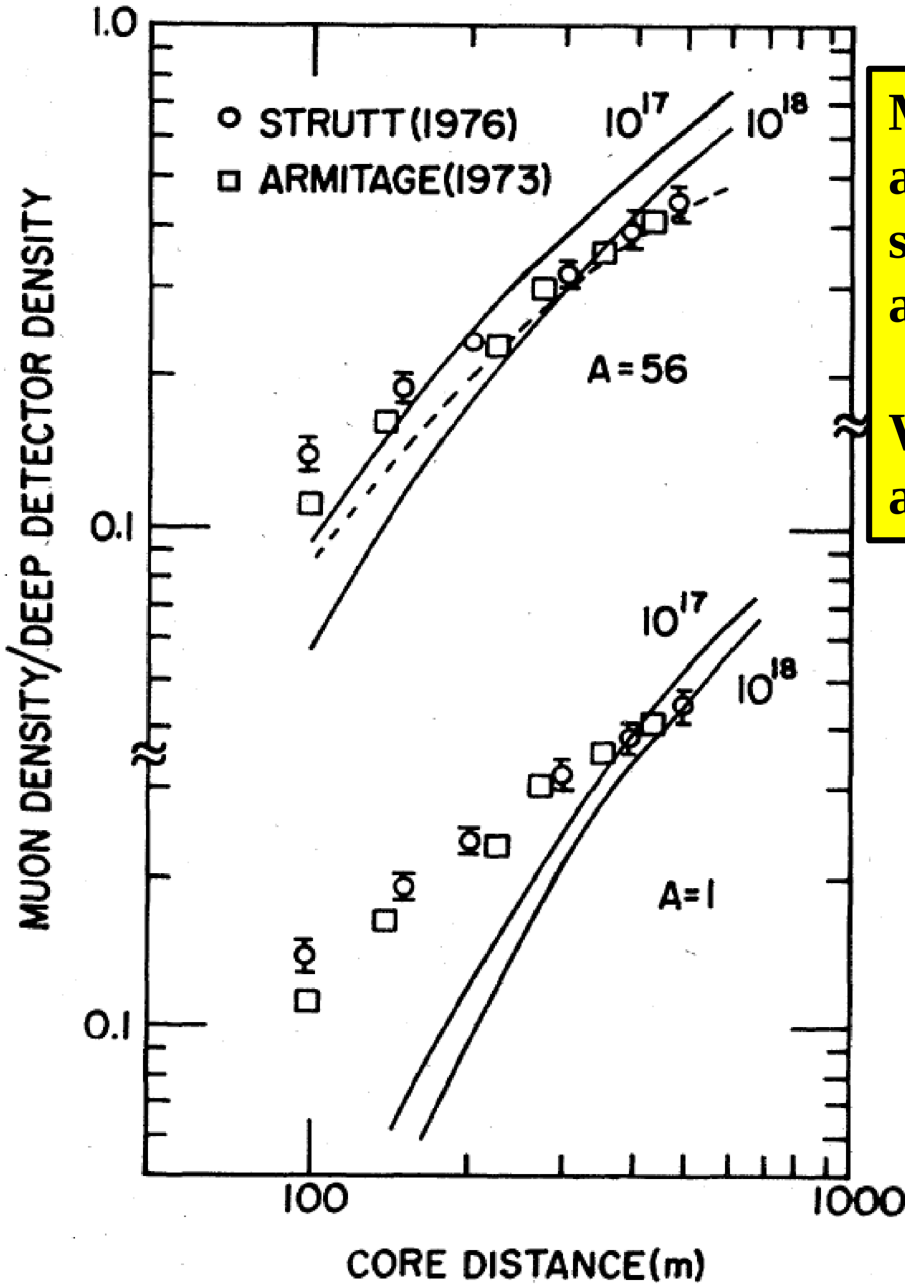

Measurements by Nottingham group at Haverah Park of muons in detectors shielded by lead – so threshold well-defined and adjacent to water-Cherenkov detectors

Wide variety of measurements of μ/Ch ratio as function of angle, distance and energy

FIG. 15. The average ratio from the response of a muon sensitive detector (threshold 0.3 GeV) to that from a deep-water Čerenkov detector at various core distances. The same data are offset to show comparison with calculations for $A = 1$ and for $A = 56$. The dashed line is an attempt to take into account a triggering bias (see text).

Yakutsk have extensive data on muons and Cherenkov light but I don't know of a description of these data that is of the quality of the description of the Akeno muon data, for example

It would really be necessary to work closely with Yakutsk people - really unsure of status of that collaboration now

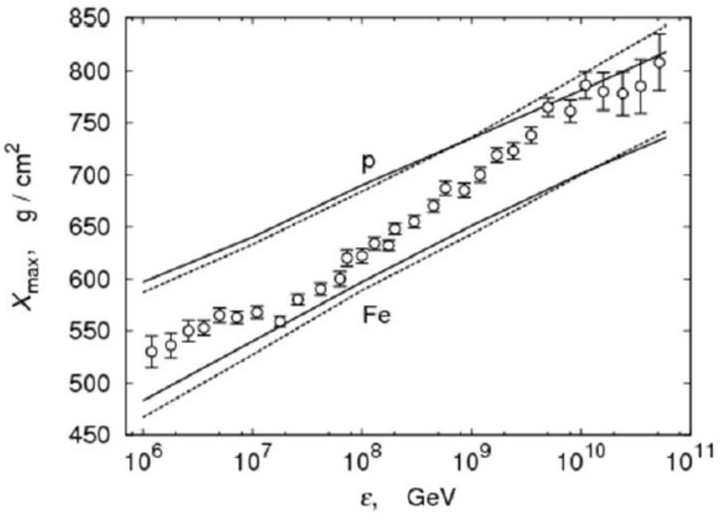

Figure 4: Dependence of X_{max} from energy. Lines are calculated values for proton and iron nuclei.

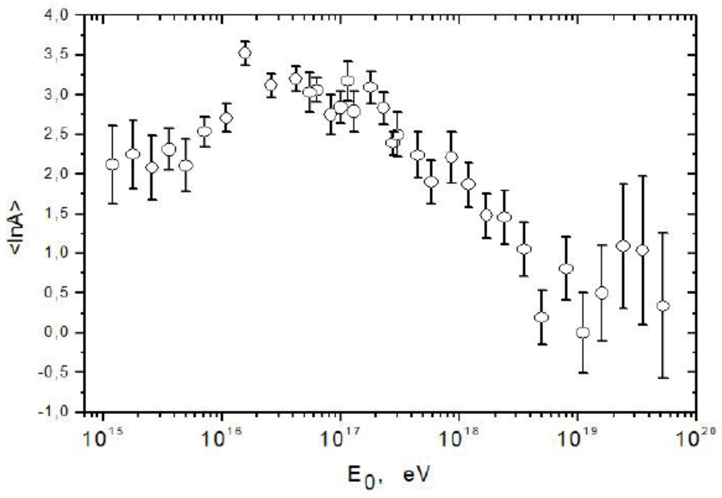

Figure 5: Mass composition of Cosmic rays highest energy are obtained at Yakutsk. Model QGSJETII-03

Petrov et al. [257], The Hague ICRC 2015

J. Phys. G: Nucl. Phys. 7 (1981) 1297–1309. Printed in Great Britain

Risetime Measurements at Haverah Park on 34 m^2

Measurement of the elongation rate of extensive air showers produced by primary cosmic rays of energy above 2×10^{17} eV

R Walker and A A Watson

Department of Physics, University of Leeds, Leeds 2, UK

Received 20 February 1981

Abstract. A measurement of the elongation rate, the rate of change of the depth of shower maximum with energy, has been made in air showers initiated by cosmic-ray primaries with energy in the range 2×10^{17}–10^{20} eV. The measurement is based on the study of the rise times of over 13 000 pulses recorded from the four 34 m^2 water Cerenkov detectors of the Haverah Park array and on an application of the elongation rate theorem.

The elongation rate is determined to be 70 ± 5 g cm^{-2} per decade, averaged over the whole energy range, while for 35 events of primary energy greater than 5×10^{18} eV the corresponding value is 40 ± 20 g cm^{-2} per decade. These results are independent of assumptions about features of high-energy interactions. The changes in mass composition, consistent with our measurement and with different assumptions about nuclear interactions, are derived.

Further, we have shown that a commonly adopted assumption used to determine the elongation rate is invalid for the case of rise time data and consequently should be tested for other parameters believed to be sensitive to shower development.

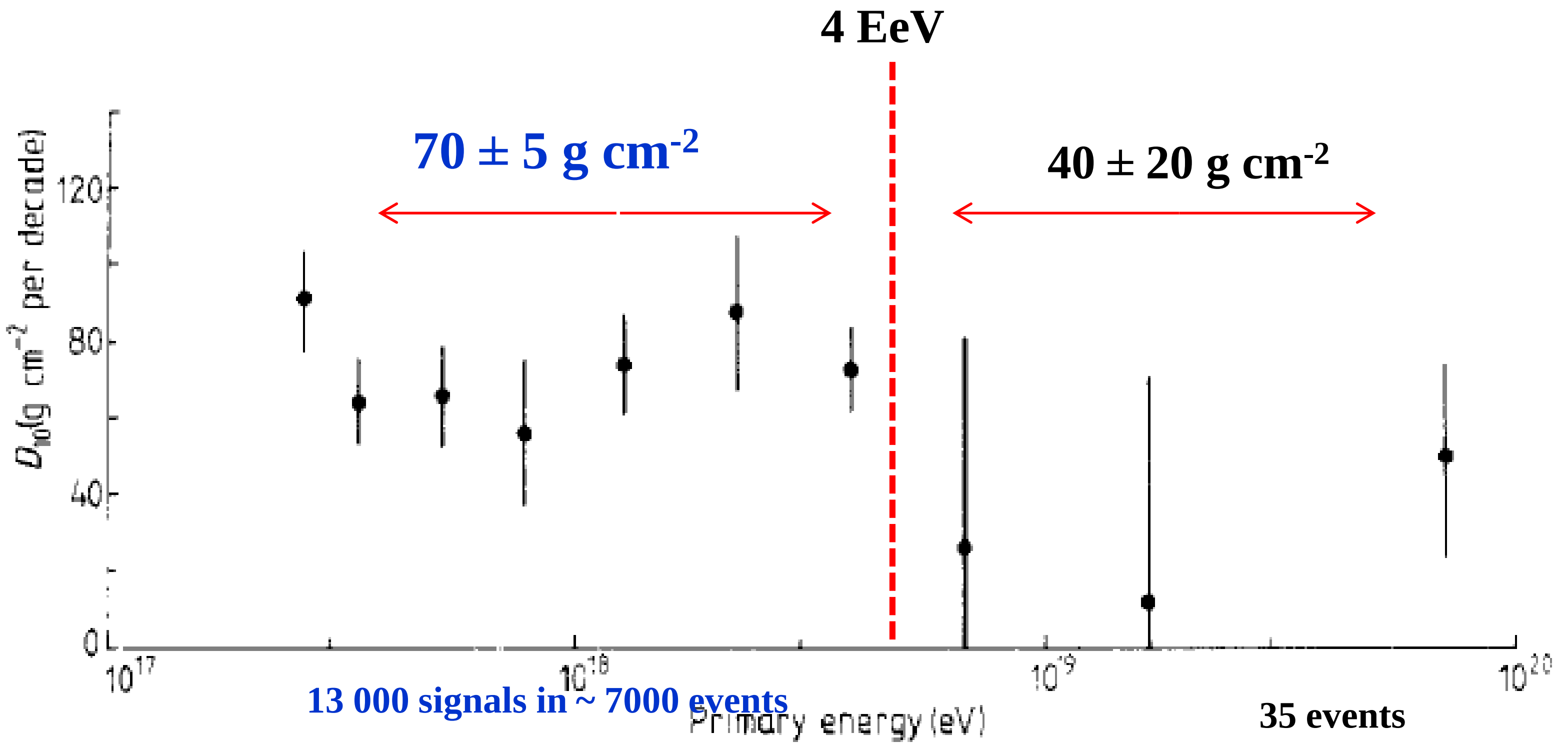

Figure 6. The elongation rate, D_{10} (g cm^{-2} per decade), as a function of primary energy. The data used to determine each point are independent. The range of energies used for each point is listed in table 2.

From model-independent analytical analysis based on Linsley's classic 1977 papers on Elongation Rate (Plovidiv ICRC 1977)

Extension to fluctuations (Walker and Watson 1982):

Assuming that $t_{1/2} = f(X - X_m)$ it is straightforward to show that

$$\sigma(X_m)_E = -\sigma(t_{1/2})_E / (\partial t_{1/2} / \partial X)_E$$

$$\sigma(E) = (250 + 2.5\ \lg^{1.8}(E/100\ \text{GeV}))\ \text{mb}$$

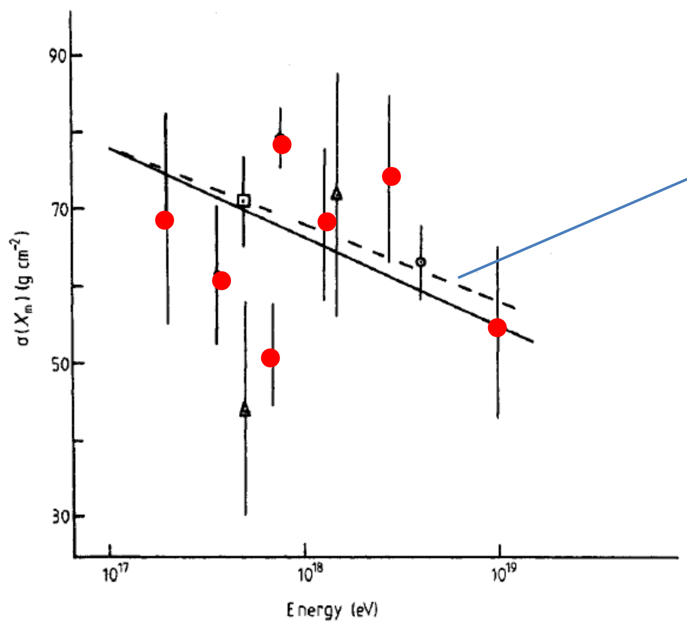

Figure 1. Variation of $\sigma(X_m)$ with energy. ♦, this paper; ⊡, Coy *et al* (1981) (see § 4); ⊙, Dyakonov *et al* (1981); △ Watson and Wilson (1974). The full line is a best fit to all 11 data points. The broken line indicates the variation to be expected for a constant mass composition and an energy-dependent cross section; it has been normalised at 10^{17} eV (see § 4 for details).

Gaisser and Yodh Ann Rev NS1980

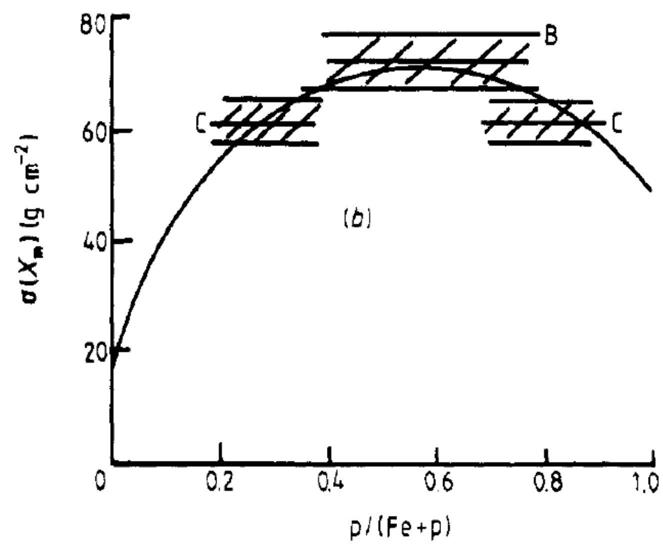

Conclusions:-

- Use Akeno data to explore muon anomaly

  – but density of concrete?

- Also use Haverah Park muon data

  LDF > 1 GeV

  μ/Cherenkov ratio as function of angle, distance and energy

  Momentum spectrum for guidance in comparisons

- Use HP LDF data to improve mass measurements

  for $0.2 \text{ EeV} < E < 2 \text{ EeV}$

- Learn more about Yakutsk data: can it be exploited?

- Use Haverah Park risetime data to test models

Back Up Slides

Linsley (1977), discussion of properties of elongation rate

$$(\partial P/\partial \ln E)|_X = -FD_e(\partial P/\partial X)|_E$$

$f(X/X_m)$, $F = X/X_m$ or $f(X - X_m)$, $F = 1$

Strong experimental evidence for F=1 from zenith dependence of

$$(\partial t_{1/2}/\partial \lg E)_X = \varepsilon = -FD_{10}(\partial t_{1/2}/\partial X)_E$$

$$(\partial P/\partial X)_E \neq (1/\bar{X}_v)(\partial P/\partial \sec\theta)_E$$

$$(\partial P/\partial X)_E = (1.4 \pm 0.2)(1/\bar{X}_v)(\partial P/\partial \sec\theta)_E$$

This was major source of systematic uncertainty

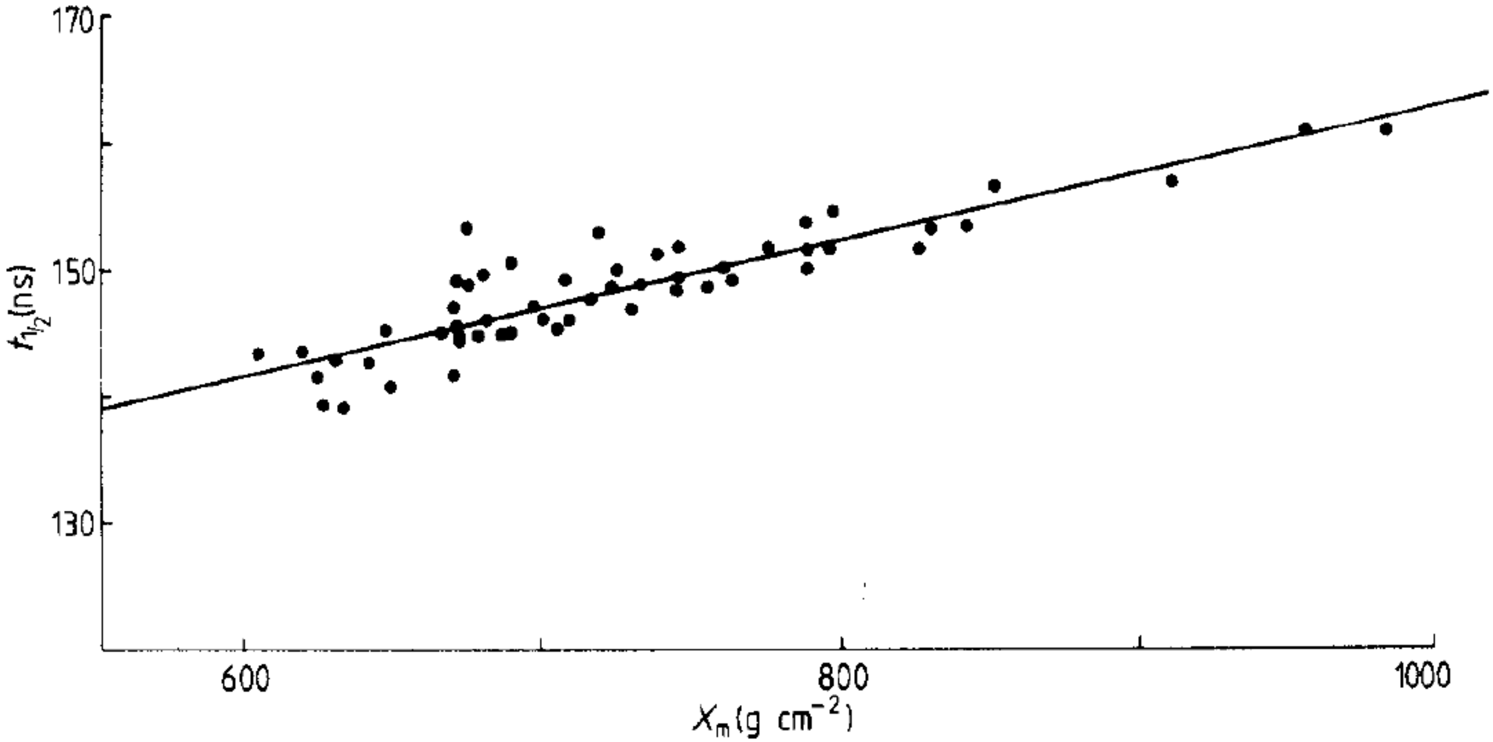

Figure 1. Calculated variation of rise time, $t_{1/2}$, at 500 m as a function of depth of maximum, X_m, for a primary proton of energy 10^{18} eV which enters the atmosphere vertically. Fluctuations in the points of interaction of the leading nucleon and of the inelasticity have been included in the calculation.

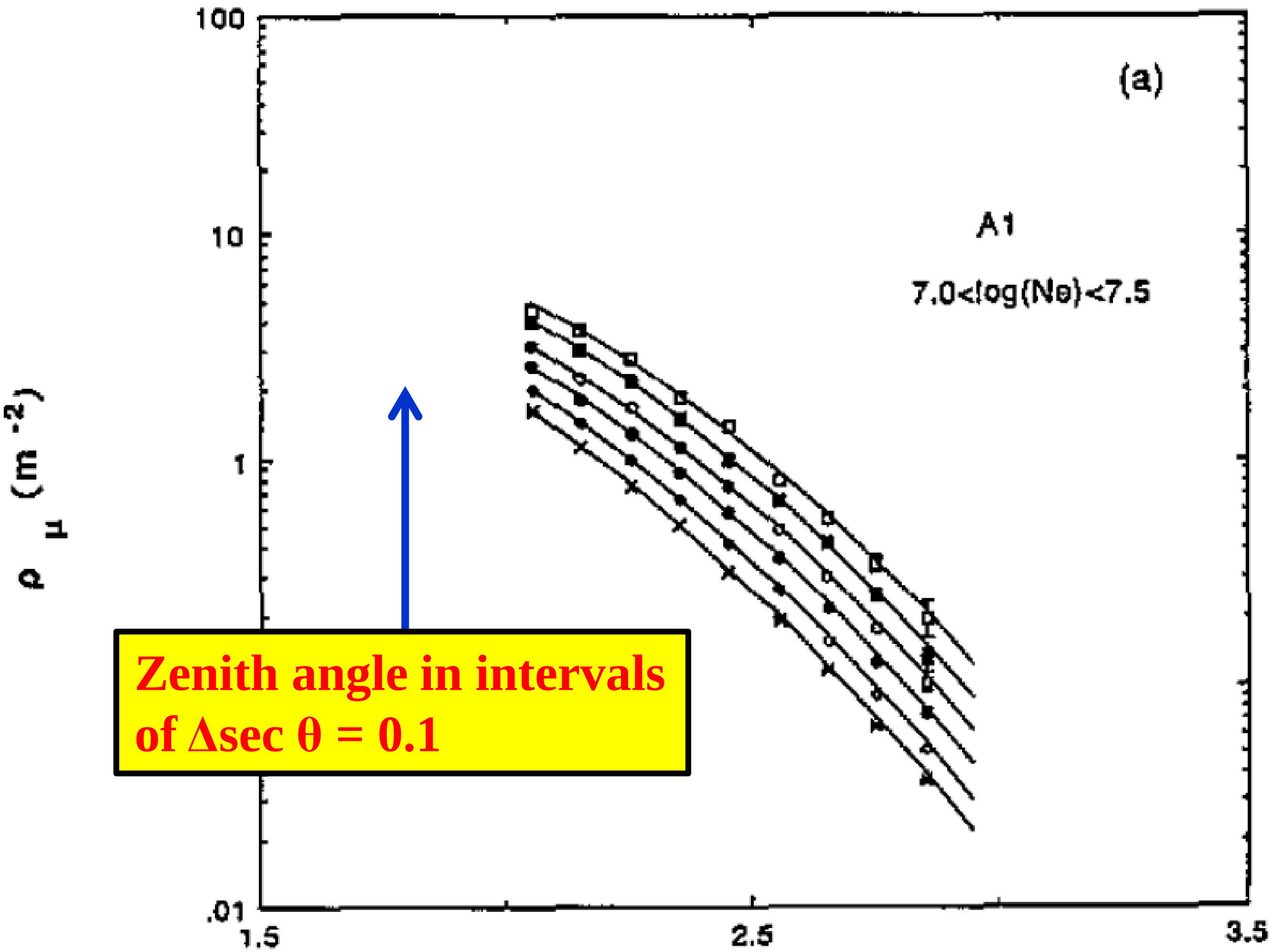

100
10
1
.01
1.5
2.5
3.5
(a)
A1
7.0<log(Ne)<7.5
ρ μ (m -2)
Zenith angle in intervals of Δsec θ = 0.1

Haverah Park (1967 – 1987)– some data may still be useful – and there have been some successes with these

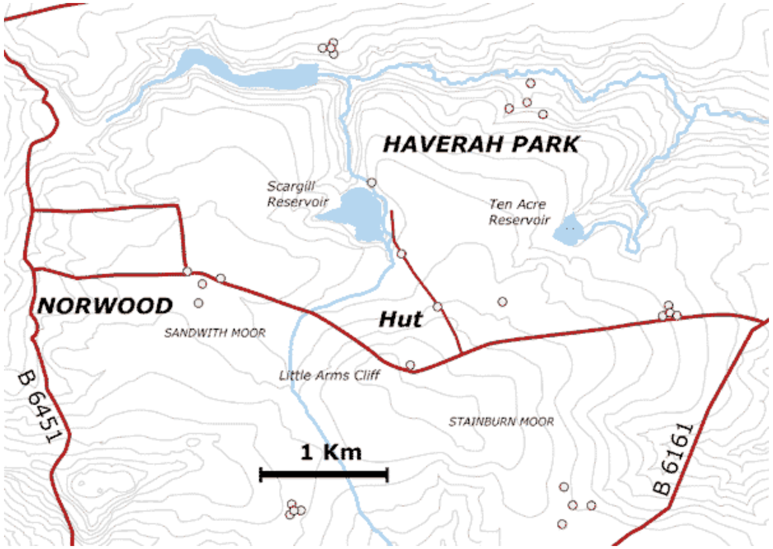

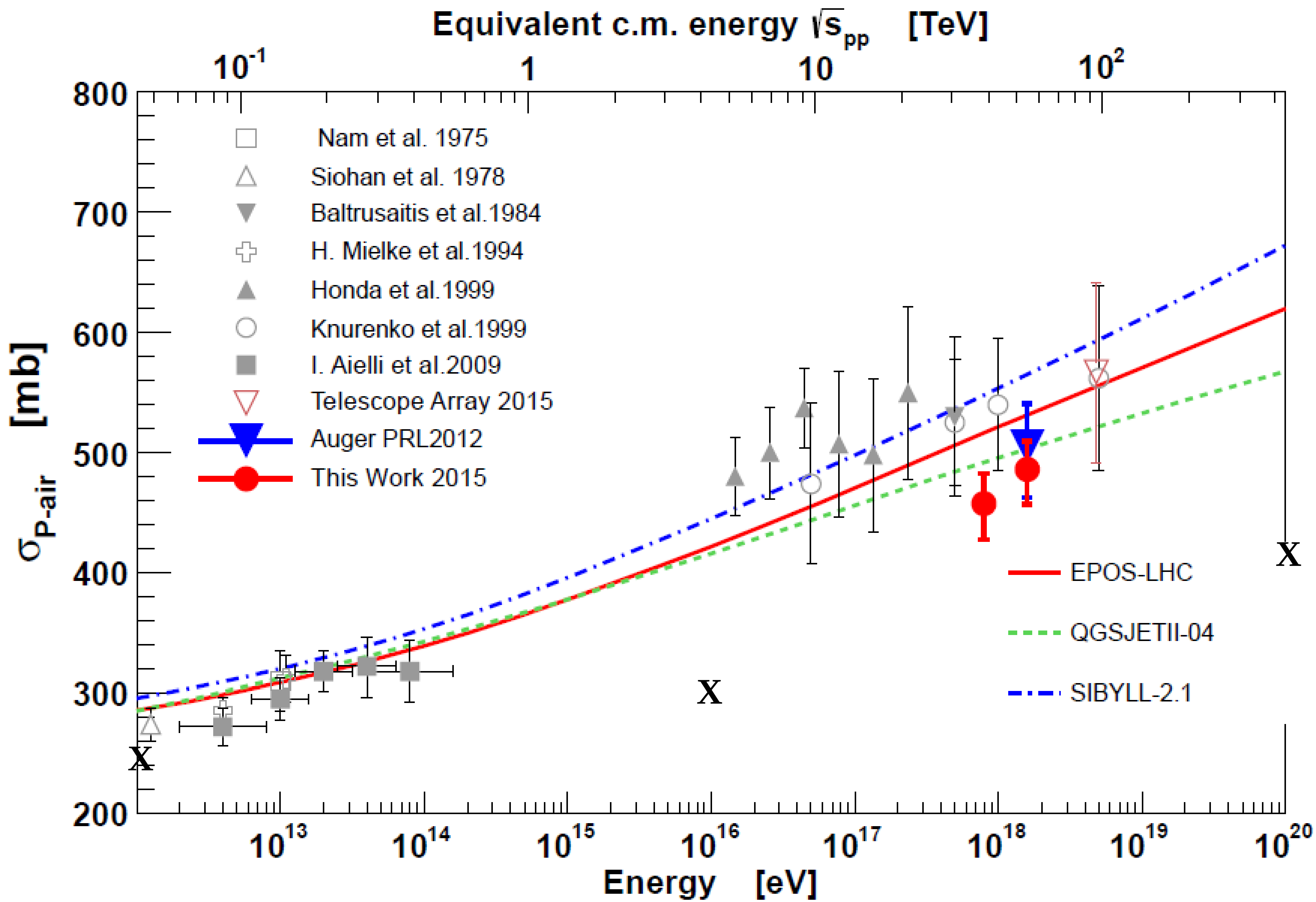

Equivalent c.m. energy $\sqrt{s}_{pp}$ [TeV]
10^{-1}
1
10
10^{2}
800
700
600
500
400
300
200
$\sigma_{P\text{-}air}$ [mb]
Nam et al. 1975
Siohan et al. 1978
Baltrusaitis et al.1984
H. Mielke et al.1994
Honda et al.1999
Knurenko et al.1999
I. Aielli et al.2009
Telescope Array 2015
Auger PRL2012
This Work 2015
EPOS-LHC
QGSJETII-04
SIBYLL-2.1
X
X
X
10^{13}
10^{14}
10^{15}
10^{16}
10^{17}
10^{18}
10^{19}
10^{20}
Energy [eV]

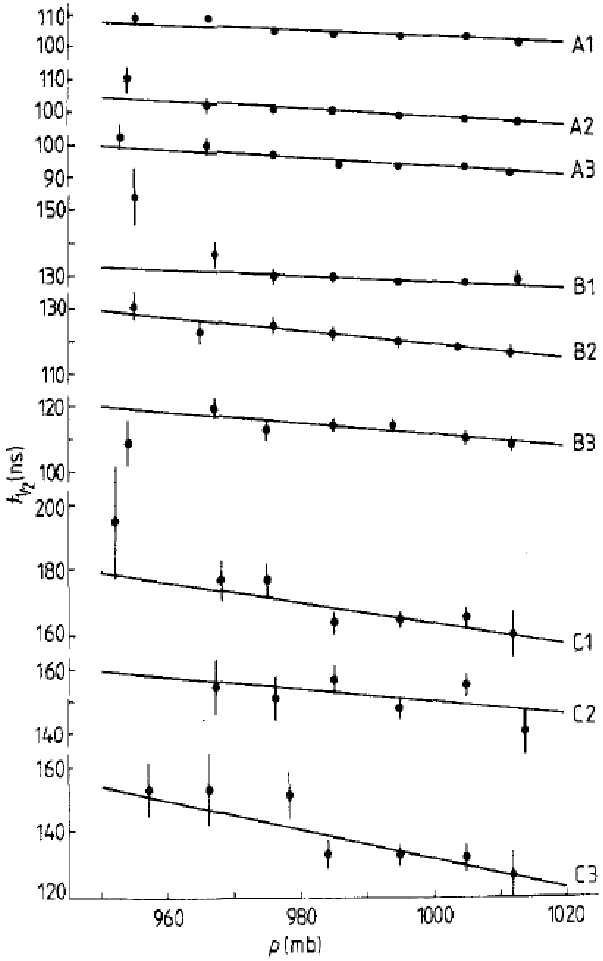

Figure 2. Variation of rise time with atmospheric pressure (mb) as a function of distance (A, 300–400 m; B, 400–575 m; C, 575–850 m) and zenith angle (sec θ) (1, 1.00–1.10; 2, 1.10–1.20; 3, 1.20–1.30).

Table 3. Comparison of the variation of $t_{1/2}$ with atmospheric depth as deduced from the pressure dependence and from the zenith angle dependence.

$\bar{r}$ (m)	$\overline{\sec\theta}$	$(\partial t_{1/2}/\partial p)_{r,\theta}$ (ns mb^{-1})	$\overline{(\partial t_{1/2}/\partial X)}_{r,\theta}$ (ns g^{-1} cm^2)	$(\partial t_{1/2}/\partial \sec\theta)_r/X_v$ (ns g^{-1} cm^2)	$\overline{(\partial t_{1/2}/\partial X)}_{r,\theta} \times [\partial t_{1/2}/(X_v \partial \sec\theta)]^{-1}$
351	1.046	-0.055 ± 0.020			
349	1.144	-0.085 ± 0.024	-0.066 ± 0.012	-0.046 ± 0.010	1.44 ± 0.41
350	1.244	-0.096 ± 0.030			
471	1.046	-0.065 ± 0.042			
472	1.146	-0.185 ± 0.046	-0.11 ± 0.02	-0.090 ± 0.010	1.22 ± 0.26
474	1.244	-0.152 ± 0.060			
663	1.047	-0.303 ± 0.123			
661	1.148	-0.168 ± 0.155	-0.28 ± 0.07	-0.16 ± 0.01	1.75 ± 0.45
660	1.243	-0.454 ± 0.138			

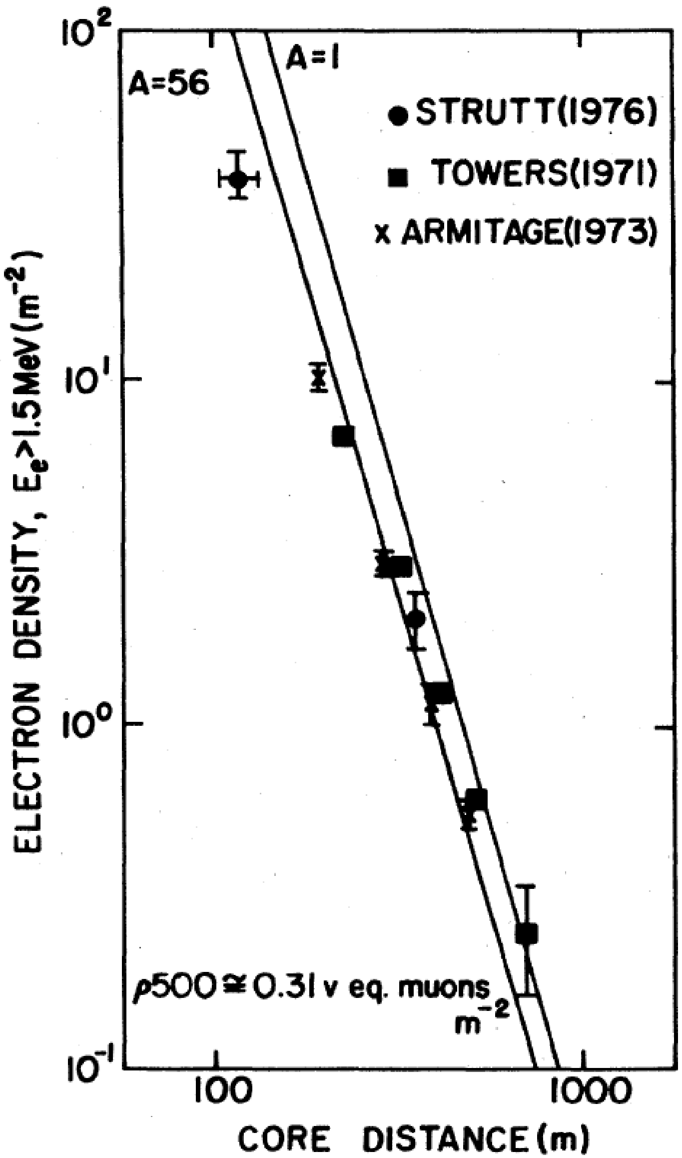

FIG. 13. The average lateral distribution of electrons (energy >4 MeV) in showers having the Haverah Park ground parameter value 0.31 m^{-2}.

TABLE I. Energies assigned to the showers observed in the Chacaltaya experiment.

Integral flux ($m^{-2}sr^{-1}s^{-1}$)	Energy derived from energy deposition by Hillas (eV)	Energy estimate from present work (eV)
10^{-6}	($\geq 1.9 \times 10^{15}$)	($\geq 1.8 \times 10^{15}$)
10^{-7}	5.9×10^{15}	7.5×10^{15}
10^{-8}	1.6×10^{16}	1.9×10^{16}
10^{-9}	5.5×10^{16}	6.5×10^{16}
10^{-10}	1.7×10^{17}	1.9×10^{17}
10^{-11}	5.5×10^{17}	5.5×10^{17}

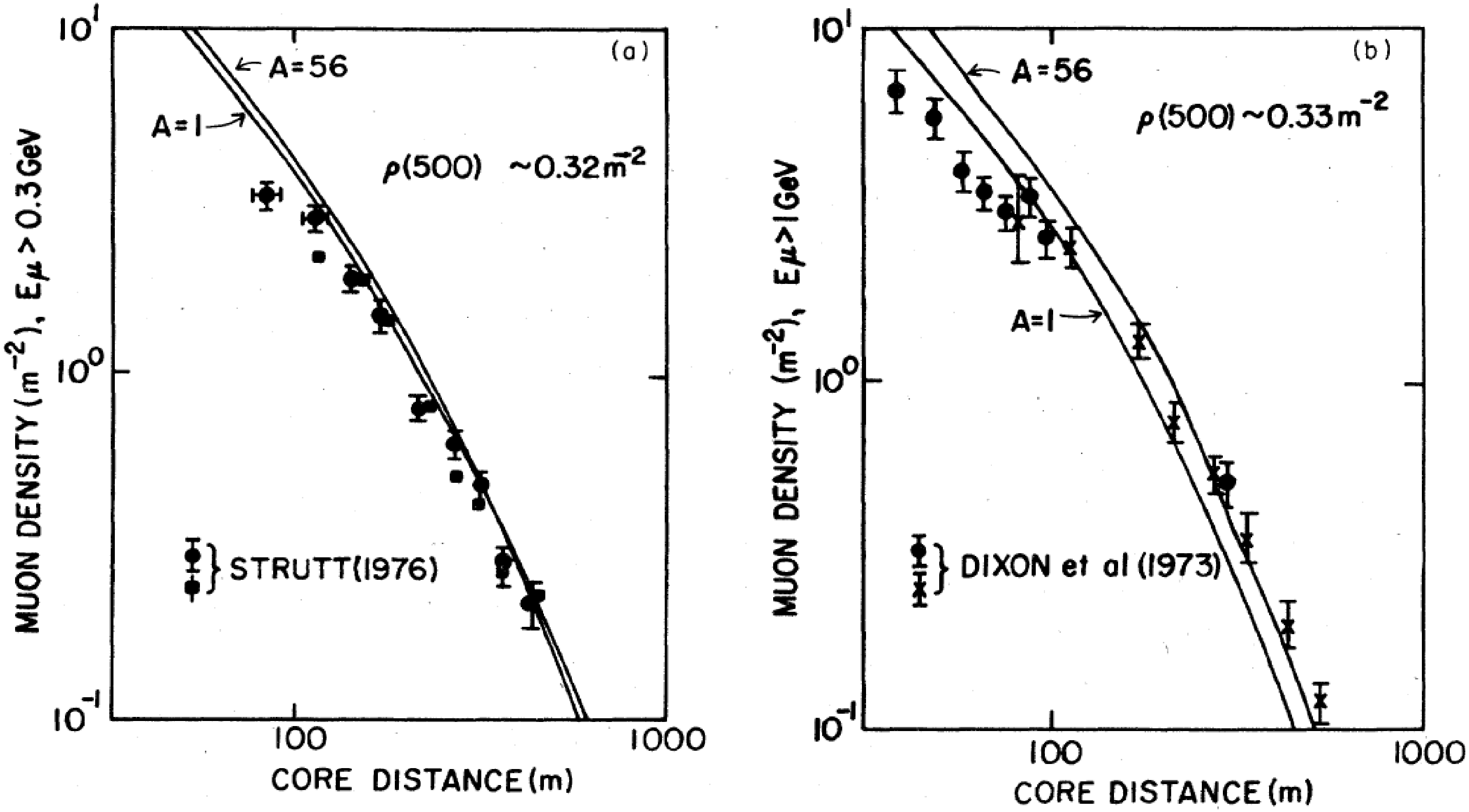

(a)
A=56
A=1
ρ(500) ~0.32m⁻²
STRUTT(1976)
MUON DENSITY (m⁻²), Eμ > 0.3 GeV
CORE DISTANCE (m)
(b)
A=56
ρ(500) ~0.33 m⁻²
A=1
DIXON et al (1973)
MUON DENSITY (m⁻²), Eμ>1GeV
CORE DISTANCE (m)

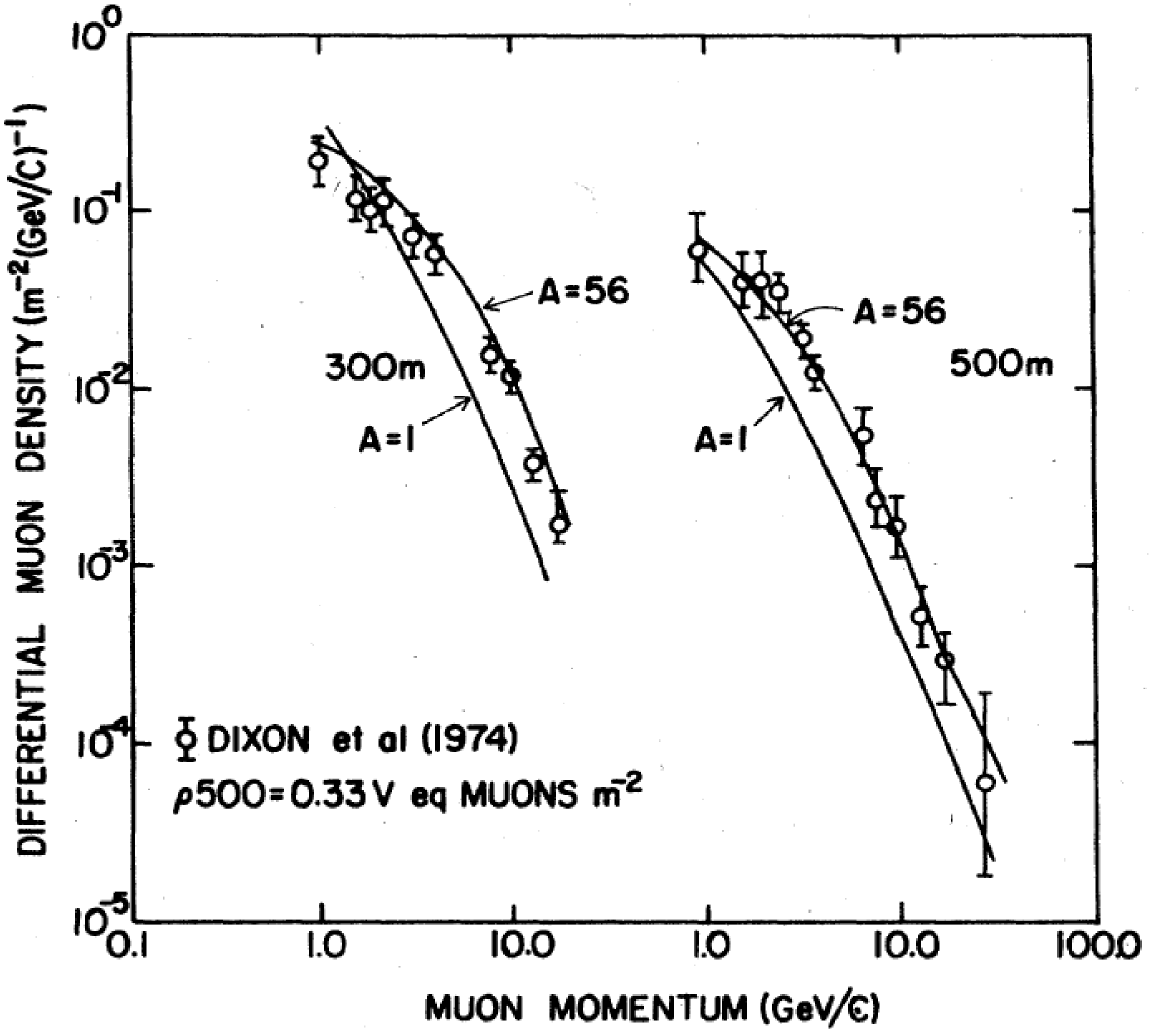

FIG. 7. The momentum spectrum of muons at 300 and 500 m from the core of showers of Haverah Park ground parameter $0.33\ m^{-2}$.

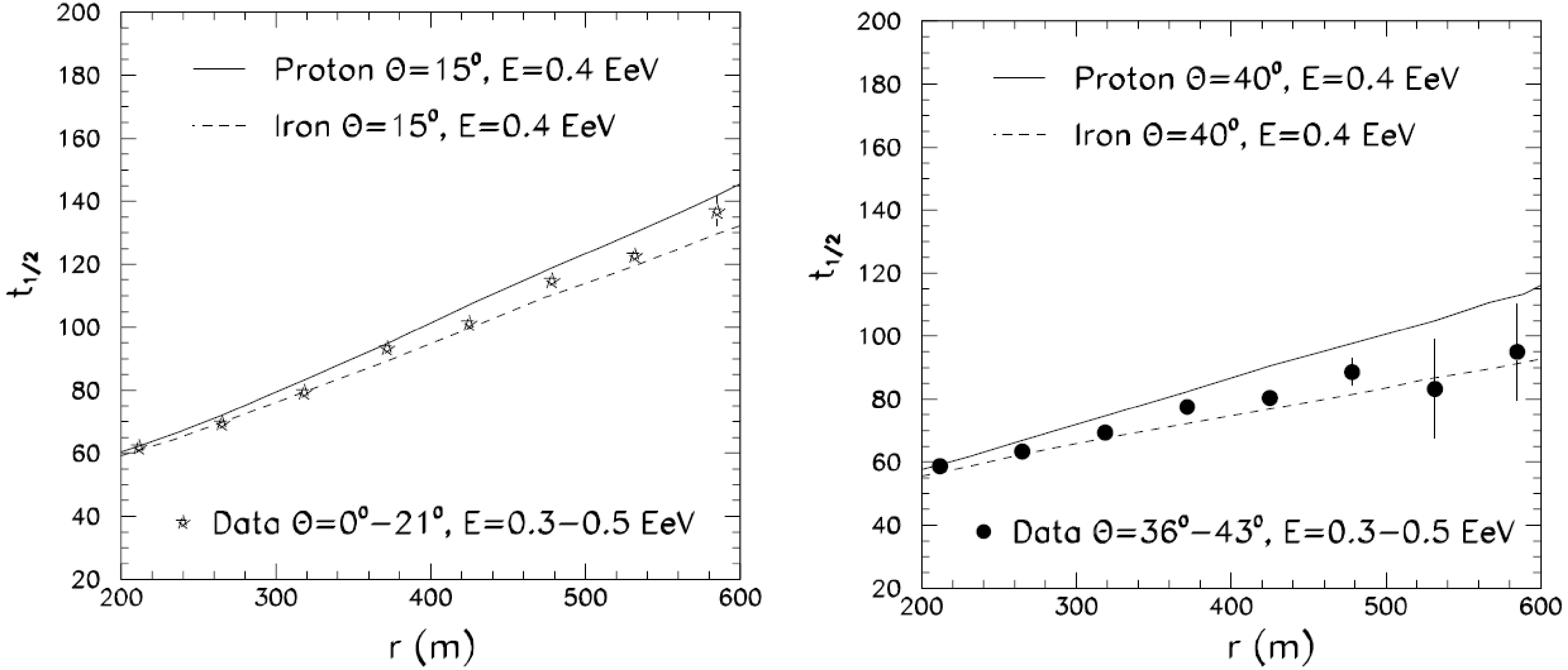

Fig. 3. Risetime versus distance to shower core as obtained in data and in simulations for proton and iron primaries.

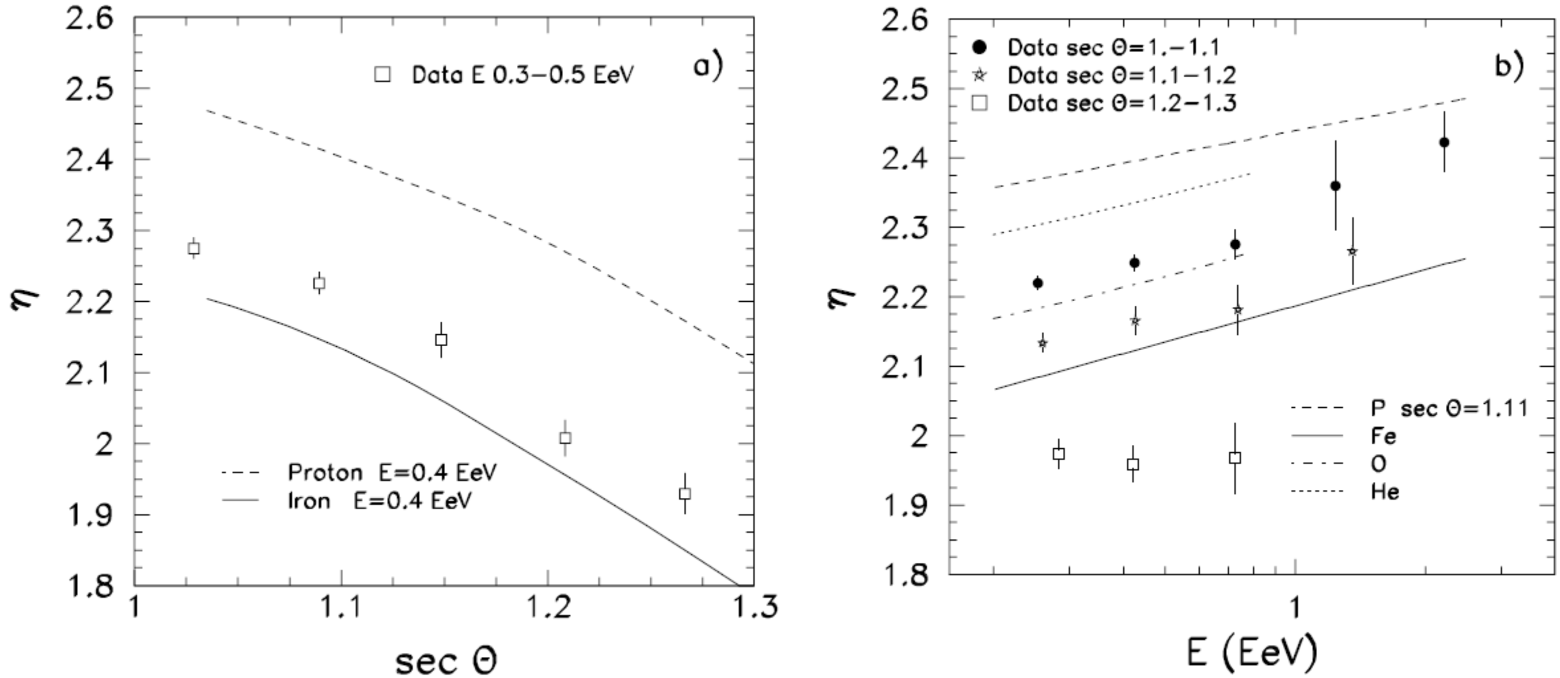

Fig. 5. Right panel: evolution of η with zenith angle; the simulation results correspond to a zenith angle of 26°, the data is binned in zenith angle bands. Left panel: evolution of η with zenith angle for data and simulations.

One of the major stumbling blocks in the search for a satisfactory theory of the origin of cosmic rays above 10^{17} eV is the limited knowledge which we have of the mass composition of the primary particles. Because the relevant parameters of particle physics are largely unknown it has proved difficult to deduce the mass composition unambiguously from available experimental data. At the present time a most promising line of attack on this problem is the study of the rate of change of the atmospheric depth of maximum shower development with energy. This rate of change has been named the 'elongation rate' by Linsley (1977). He has shown how the elongation rate depends explicitly on particle physics and has demonstrated how this feature can be exploited to make efficient use of experimental data. The major result of Linsley's paper was discovered independently by Shibata (1977) and by Hillas (1978), but these authors did not discuss its practical applications. Extensions to Linsley's result have been outlined by himself and others (Linsley 1979, Gaisser *et al* 1979, Linsley and Watson 1981) and are discussed in § 2.